



Available online at [scholarcommons.usf.edu/ijis](https://scholarcommons.usf.edu/ijis)

# International Journal of Speleology

Official Journal of Union Internationale de Spéléologie



## Hypogenic caves of Syracuse area, Sicily (Italy): geomorphological evidence of CO<sub>2</sub> degassing, fresh-salt water mixing, and late condensation corrosion

Philippe Audra <sup>1</sup>, Jean-Yves Bigot<sup>2</sup>, Didier Cailhol <sup>3</sup>, Pierre Camps <sup>4</sup>, Ilenia M. D'Angeli <sup>5</sup>, R. Lawrence Edwards <sup>6</sup>, Fernando Gázquez-Sánchez <sup>7</sup>, Hai Cheng <sup>8</sup>, Gabriella Koltai <sup>9</sup>, Giuliana Madonia <sup>10</sup>, Jean-Claude Nobécourt<sup>2</sup>, Marjan Temovski <sup>11</sup>, Marco Vattano <sup>10</sup>, and Jo De Waele <sup>12</sup>

<sup>1</sup>Polytech'Lab - UPR 7498, Polytech Nice Sophia, Université Côte d'Azur, 930 route des Colles, 06903 Sophia-Antipolis, France

<sup>2</sup>Association française de karstologie, France

<sup>3</sup>Laboratoire Traces, Université Toulouse Jean Jaurès, Toulouse, France

<sup>4</sup>Géosciences Montpellier, Université de Montpellier, CNRS, 34095 Montpellier Cedex 05, France

<sup>5</sup>Department of Geosciences, University of Padova, Via Gradenigo 6, Padova, Italy

<sup>6</sup>University of Minnesota, Department of Earth Sciences, 3 Morrill Hall, 100 Church St. S.E., Minneapolis MN 55455, USA

<sup>7</sup>Department of Biology and Geology, University of Almería, 04120, La Cañada de San Urbano, Almería, Spain

<sup>8</sup>Institute of Global Environmental Change, Xi'an Jiaotong University, Xi'an 710054, China & Key Laboratory of Karst Dynamics, MLR, Institute of Karst Geology, CAGS, Guilin 541004, China

<sup>9</sup>Institute of Geology, University of Innsbruck, Innrain 52, 6020 Innsbruck, Austria

<sup>10</sup>Department of Earth and Marine Science, University of Palermo, Via Archirafi 20-22, 90123 Palermo, Italy

<sup>11</sup>Isotope Climatology and Environmental Research Centre (ICER), HUN-REN Institute for Nuclear Research (ATOMKI), Bem tér 18/C, H-4026 Debrecen, Hungary

<sup>12</sup>University of Bologna, Department of Biological, Geological and Environmental Sciences, Via Zamboni 67, 40126, Bologna, Italy

### Abstract:

Many caves in Sicily have been shown to have a sulfuric acid or other hypogenic origin. We studied three caves (Palombara, Scrivilleri, Monello) near Syracuse (eastern Sicily), in an area that was strongly uplifted and faulted, creating multiple Pleistocene marine terraces. Mineralogy, stable isotopes and dating methods (paleomagnetism, U/Th) were used to characterize cave sediments, some of which were related to the initial hypogenic phase (Fe and Mn oxides, calcite spar), others were introduced by surface runoff later. Many other sediments are the result of in situ weathering, such as lime sands produced by condensation-corrosion processes on the calcarenite walls. Phosphates, kaolinite and montmorillonite are related to bat guano decay. Stable isotopes show that the speleothems derive from surface seepage with temperatures similar to the present, with no evidence of a hydrothermal origin. Other deep sources of aggressivity are also excluded. We obtained an age of 603 ka for a marine notch deposit near Palombara, as well as a possible paleomagnetic inversion (>780 ka) for clastic allogenic sediments. These ages are discussed, raising the question of the reliability of calculations extrapolated from marine terrace dating and the possibility that the caves may be older than expected. Cave morphologies clearly indicate a hypogenic phase, with aggressive ascending flows creating the typical Morphologic Suites of Rising Flow (MSRF). The bubble trails and acid notches are formed by carbonic degassing and subsequent acidification in more or less closed aerated environments at the water table. Carbon dioxide probably derived from both the bedrock and the oxidation of surface-derived organic carbon at the density boundaries of the freshwater lens. We propose a mixed Flank Margin Cave and hypogenic speleogenesis model, where dissolution was favored in areas of greater CO<sub>2</sub> concentration, producing phreatic maze patterns recording past sea-level positions. We suggest that aggressiveness of the rising fluids could have partly originated at a shallow depth, in the mixing zone between fresh and salt water.

### Keywords:

Carbonic degassing, hypogenic speleogenesis, flank margin caves, Palombara Cave, Scrivilleri Cave, Monello Cave

Received 25 May 2024; Revised 12 August 2024; Accepted 13 August 2024

### Citation:

Audra, P., Bigot, J.-Y., Cailhol, D., Camps, P., D'Angeli, I.M., Edwards, R.L., Gázquez-Sánchez, F., Cheng, H., Koltai, G., Madonia, G., Nobécourt J.-C., Temovski, M., Vattano, M., De Waele, J., 2024. Hypogenic caves of Syracuse area, Sicily (Italy): geomorphological evidence of CO<sub>2</sub> degassing, fresh-salt water mixing, and late condensation corrosion. *International Journal of Speleology*, 53(2), 211-234. <https://doi.org/10.5038/1827-806X.53.2.2516>

## INTRODUCTION

Over the last twenty years karstologists worldwide have discussed the origin of caves and are now widely considering two types of karst: epigenic and hypogenic. Epigenic karst is unconfined, and water is recharged from the directly overlying land surface. Hypogenic karst, on the contrary, is generally confined and water enters the soluble units from below (Klimchouk et al., 2000; Ford & Williams, 2007). Hypogenic waters can derive from truly deep sources (e.g., magmatic fluids) but more commonly can also be deeply looping surface-derived waters that have since long lost most of their typical epigenic geochemical imprint. Klimchouk (2007) defines hypogenic speleogenesis as “the formation of caves by water that recharges the soluble formation from below, driven by hydrostatic pressure or other sources of energy, independent of recharge from the overlying or immediately adjacent surface”. Palmer (2000) gives a broader definition: “hypogenic speleogenesis involves water in which the aggressiveness has been produced at depth beneath the surface, independent of surface or soil CO<sub>2</sub> or other near-surface acid sources”, or “involves epigenic acids rejuvenated by deep-seated processes” (Palmer, 1991). According to Klimchouk’s definition flank margin caves created by the mixing of saline and fresh water in coastal settings would not be truly hypogenic, nor would the caves formed by oxidation of sulfides by descending waters, as in both cases there is no exclusively rising flow involved. Palmer’s definition works well in most rocks, whereas Klimchouk’s vision is based more on hydrological concepts rather than on the chemistry involved.

An increasing body of evidence suggests that many caves formed by hypogenic processes, implying the upward recharge from a deep route rather than epigenic input (Klimchouk, 2007), or the formation of renewed aggressivity at depth (Palmer, 2000). Generally, these rising fluids are rich in CO<sub>2</sub> and/or H<sub>2</sub>S, and can be sourced from deep hydrothermal activity (De Waele & Gutiérrez, 2022).

Flank margin caves (FMC) are dissolution caves in carbonate rocks developing along many coastal karst areas. They are characterized by morphological indicators of diffuse flow, such as cupolas, smooth ceiling channels, thin rock partings, random connection between adjacent rooms, and spongework morphologies (Klimchouk et al., 2014). Following Palmer’s definition these can be classified as hypogene karst, since diffusely flowing water acquires its aggressivity by mixing of different fluids, below the surface, isolated from direct hydrologic connection with surface hydrology (Mylroie & Mylroie, 2009). FMC form by mixing dissolution processes in the distal margin of the freshwater lens, under the flank of the enclosing landmass (Mylroie & Carew, 1990), and by the production (or arrival) of CO<sub>2</sub> and/or H<sub>2</sub>S from both more or less distant surface and/or deep sources (Bottrell et al., 1993; Gulley et al., 2015; López-Martínez et al., 2020; Breithaupt et al., 2022). Their development is controlled by the position of the fresh water lens, which in turn, is connected to sea-

level elevation (Fratesi, 2013; Mylroie, 2013).

FMC were initially described from diagenetically immature young carbonate coasts such as those occurring in the Bahamas (Mylroie & Carew, 1990). The high primary porosity of these rocks favors diffuse flow and the formation of irregular globular rooms, dead-end passages, and phreatic slow-flow morphologies (spongework). FMC also develop in diagenetically more mature and crystalline carbonate rocks, and water flow is guided mainly by the most permeable pathways, determined by joints, faults, and bedding planes (Mylroie et al., 2008; Otoničar et al., 2010; Mylroie & Mylroie, 2013; Ruggieri & De Waele, 2014; D’Angeli et al., 2015). Morphologies of cave passages indicate slow flow conditions (e.g., absence of scallops), and most sediments are autogenic (absence or very scarce presence of allogenic deposits).

We describe three cave systems in the Syracuse area eastern Sicily, with distinct morphologies indicative of rising flow, sea-level stillstands, and upwelling CO<sub>2</sub>. The aim is to understand their relationships with the marine terraces, their relative age, and their speleogenetic framework.

### Synthesis of previous works in Sicilian hypogenic caves

The hypogenic caves of Sicily have been the subject of several publications by the authors of this article. These papers were synthesized in Vattano et al. (2017). Acqua Fitusa (San Giovanni Gemini, Agrigento province) and Acqua Mintina (Butera, Caltanissetta province) caves are outstanding examples of sulfuric acid speleogenesis (Vattano et al., 2012; De Waele et al., 2016; Lugli et al., 2017; D’Angeli, 2019; D’Angeli et al., 2019a); Eremita and Cocci caves (Mt. Inici, Castellammare del Golfo, Trapani province) owe their origin to rising hydrothermal flow (Vattano et al., 2012; Audra et al., 2012; Di Maggio et al., 2012; Vattano et al., 2013a; De Waele et al., 2014). Monte Kronio System is still actively evolving through thermal vapor (Vattano et al., 2013b; Badino & Torelli, 2014; Di Piazza et al., 2017; Vattano et al., 2017). Vento shaft (Abisso del Vento, Isnello, Palermo province), which is also probably a hypogenic cave (Vattano et al., 2017) has typical red residual material (Aricò & Vattano, 2007). Personaggi Cave displays the typical Morphologic Suite of Rising Flow (MSRF), sensu Klimchouk (2007, 2009), with a maze pattern, feeders, rising channels, cupolas, etc. (Audra et al., 2015; Vattano et al., 2015). Most caves show late stages of significant passage enlargement and reshaping through condensation-corrosion often related to sulfuric processes and/or the presence of strong thermal gradients. In addition, the presence of bat colonies and guano strongly enhance condensation-corrosion and cave expansion (Cailhol et al., 2019; Audra et al., 2021). Guano decay produces a large variety of minerals, mainly phosphates and secondary sulfates such as gypsum (Audra et al., 2019), with a special mineralogy in salt-water influenced FMCs (Onac et al., 2001). Sulfate minerals from sulfuric speleogenesis have been widely investigated, making it possible to date speleogenesis phases, to determine uplift rates, and to analyze

geomorphic evolution (Polyak et al., 1998; Piccini et al., 2015, D'Angeli, 2019; D'Angeli et al., 2018, 2019b; Polyak et al., 2022; Temovski et al., 2023; De Waele et al., 2024). Among the Sicilian caves, those from the Syracuse area were the least investigated hypogenic caves, with the exception of one cave mentioned in Vattano et al. (2017). As background, the caves of this area are described as speleological objects in a detailed study by the Centro Ibleo di Ricerche Speleo-Idrologiche (CIRS) (Ruggieri & Amore, 2000; Ruggieri & Zocco, 2000; Ruggieri et al., 2000).

### Syracuse caves

Most of the caves in the Syracuse area develop in Miocene calcarenites and appear to be correlated with Pleistocene marine terraces. These caves feature a subhorizontal maze pattern interspersed with a few short vertical tracts, both constrained by the fracture network and lithologic differences. Furthermore, they are not directly linked to surface water infiltration or rapid flow, and do not contain corresponding fluvial sediments. On the contrary, these caves display phreatic morphologies typical of slow upward flows, and wall features associated with CO<sub>2</sub> degassing. For these reasons, they resemble hypogenic caves, and the context suggests that they could be abandoned Flank Margin Caves (FMC) associated with the former mixing of fresh and salt waters draining surface flow towards ancient sea levels evidenced by marine terraces. In this article, we study the geologic and geomorphologic setting of the karstified calcarenites of the Syracuse area subject to strong uplift, as well as the morphology and sediments of these atypical caves, in order to deduce the types of speleogenesis and the setting in which they may have formed.

## GEOLOGY

### Sicilian geodynamic context

Sicily represents a segment of the Apennine-Tyrrhenian System, linked to the convergence of the African and Eurasian plates and the Ionian lithosphere subduction, lying in one of the most active zones in the Mediterranean (Doglioni et al., 1999; Faccenna et al., 2004; Chiarabba et al., 2008). Three regional elements have been recognized in the Sicilian continental subduction complex (Lentini et al., 1994; Catalano et al., 2013; Butler et al., 2019): a) the south to southeast-verging Sicilian Fold Thrust Belt (FTB) formed since the Middle Miocene; b) the Late Pliocene-Quaternary foredeep (Gela foredeep), in the footwall of the frontal sector of the thrust belt, in southern Sicily and its offshore; c) the Hyblean-Pelagian foreland belonging to the African plate (Sulli et al., 2021). The Hyblean Plateau pertains to the Pelagian Block, or Malta Platform (Lentini & Carbone, 2014), and represents the northernmost emerged part of the African foreland plate (Fig. 1A). The Hyblean Plateau has been interpreted as a positive flexural bulge originated by the load of the SE-verging Sicilian FTB (Billi et al., 2006; Pedley & Grasso, 1992) and as a consequence of intraplate tectono-magmatic processes (Henriquet et al., 2019). During the

Pleistocene, the Hyblean Plateau uplift became more pronounced, with the Plateau tilted to the SE, then fragmented by NW-SE subsident basins (Pavano et al., 2022). Uplift accelerated during the Middle Pleistocene, resulting in NNW-SSE faulting along the eastern coast (i.e., Avola Fault). This coastline is thus bounded by active normal faults, extending offshore through the Hyblean-Maltese escarpment, and culminating in the Siculo-Calabrian Rift Zone, whose current extension rate reaches 3.6 mm/yr (Catalano et al., 2010). This active zone is responsible for numerous destructive historical earthquakes and tsunamis, as well as for the intense activity of Mount Etna (De Martini et al., 2012).

### Geologic structure of the Syracuse area

The study area is located at the eastern foot of the Hyblean Plateau bordering the Ionian Sea (Fig. 1A, 1B). The Augusta and Florida basins correspond to Pleistocene grabens, bounded by NW-SE normal faults (Monti Climiti Fault, N. and S. Syracuse faults, Spinagallo Fault; Fig. 1C). These basins are separated by horsts: to the N the Monti Climiti - Belvedere - Santa Panagia horst, forming an isthmus of the Hyblean carbonate plateau tilted to the ESE, and to the S, beyond the Florida basin, is the Canicattini-Cassibile horst (Catalano et al., 2010). The latter borders the coastal plain and is bounded to the SE by the Avola Fault (shown in Figure 1B). The NW-SE faults delimiting the basins were active in the Plio-Pleistocene before about 400 ka ago, forming escarpments, 170 m high and degraded by erosion for the E. Climiti Fault, 300 m for the W. Climiti Fault, and 150 m for the Spinagallo Fault (Catalano et al., 2010). On the other hand, the NE-SW Avola Fault, which borders the coastal plain with a "fresh" escarpment up to 290 m high displaying trapezoidal facets, indicates more recent activity, mostly post-dating 400 ka. The Avola Fault is associated with the offshore activity of the Malta escarpment parallel to the coastline, epicenter of the destructive 1693 earthquake (M7) (Piatanesi & Tinti, 1998; Bianca et al., 1999).

### Lithology

The Hyblean Plateau corresponds to the emerged part of the foreland domain. It comprises the Meso-Cenozoic sedimentary cover of the African margin, starting with Triassic rocks encountered only in boreholes (Lentini & Carbone, 2014). In the eastern Hyblean area, Upper Cretaceous volcano-sedimentary deposits outcrop, followed by Cretaceous-Oligocene platform and margin carbonates, and by an Oligo-Miocene lagoonal carbonate sequence ending in Tortonian volcanics (Fig. 1). This last carbonate sequence, the Monti Climiti Fm. (Mc in Figures 1B, 1C), in which the studied caves are located, is over 300 m thick. It consists of the Melilli Member at the base, which is a white calcarenite that becomes more marly at the top, followed by the Syracuse Limestone Member, an algal calcarenite with bryozoans and echinoderms. The sequence continues through the Tortonian limestones with the first signs of volcanic rocks and ends in the Lower Messinian with the

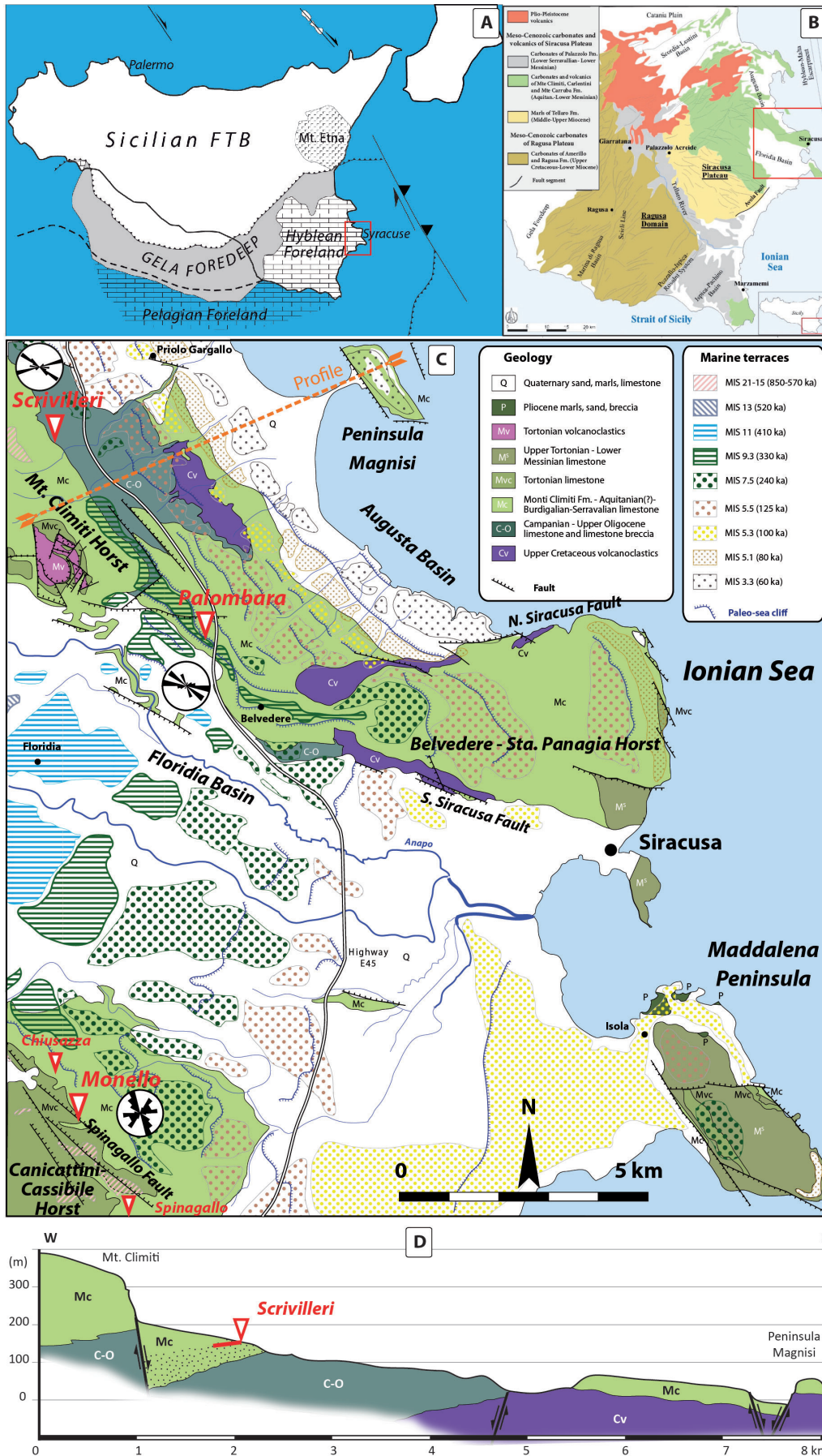


Fig. 1. Geologic setting. A) Main elements of the collisional complex of Sicily (Sicilian FTB, Sicilian Fold and Thrust Belt - data compiled from various Authors — e.g., Catalano et al., 2013 — modified and simplified). B) Stratigraphic-structural scheme of the Hyblean plateau (Distefano et al., 2021, adapted from Lentini & Carbone, 2014). The red frame indicates the study area shown in Figure 1C. C) Geologic map of the Syracuse area with the 3 studied caves (large red triangle) and 2 mentioned caves (small triangles). Colored areas show lithologic outcrops; hatchings show marine terraces with corresponding Marine Isotope Stage (MIS) and their age in thousands of years (ka). Rose diagrams correspond to the fracture frequency measured in caves and are shown close to the corresponding caves. Profile to the NW is shown on Figure 1D. Geology after Grasso et al. (1987); marine terraces after Catalano et al. (2010), Pavano et al. (2019). D) Geologic profile showing the Miocene sediments at the foot of Monti Climiti (modified from Lentini & Carbone, 2014). Same keys as in C. The profile location is shown in C. Scrivilleri cave extension is shown in red.

marly-limestone of the Monte Carrubba Fm. The area emerged during the Messinian Salinity Crisis, and remained in continental conditions during the Pliocene lacking deposition of the blue marine marls of the Trubi Fm. Only the basins formed by vertical movements in the Upper Pliocene, were filled with Quaternary deposits, mainly composed of calcarenites and marine silts.

### Series of marine terraces

Due to the strong and continuous regional uplift of the eastern Hyblean coastline (Antonioli et al., 2006), the position of past sea levels has been recorded by a series of stepped marine terraces, making Sicily an exceptional model for quantifying Quaternary uplift rates. The highest terrace, tilted and now perched between 450 and over 600 m in altitude, is considered to be a wavecut platform.

In the Syracuse area, as on the entire Sicilian east coast and as far as Calabria, the marine terraces are well-marked in the form of gently sloping abrasion platforms delimited landward by paleo-cliffs that are clearly visible in the landscape, or by stacked notches along fault escarpments, as in the Spinagallo Cave. Overall, the maximum uplift is recorded further NE of Sicily, on the northern tip of Mount Etna, notably by the MIS 5 terraces (Antonioli et al., 2006; Bonforte et al., 2015; Pavano et al., 2019; Meschis et al., 2020). Uplift tends to decrease towards the South, reaching stability around Capo Passero at the SE tip of Sicily.

Early work at the foot of the Monti Climiti and in the Quaternary Florida basin established a relative chronology of marine terraces on the Syracuse isthmus (Carbone et al., 1982; Di Grande & Raimondo, 1982). Subsequent studies used Electron Spin Resonance (ESR), Amino Acid Racemization (AAR)/Isoleucine Epimerization (IE), radiocarbon ( $^{14}\text{C}$ ), and U-series (U/Th) dating, on various materials including paleontological remains, marine and fluvial sediments, and submerged speleothems (data and discussion in Bada et al., 1991; Bianca et al., 1999; Marziano & Chilardi, 2005; Antonioli et al., 2006; Scicchitano et al., 2008; Dutton et al., 2009; Catalano et al., 2010; Spampinato et al., 2011; Bonfiglio et al., 2022; Meschis et al., 2022). The main dated landmarks are located between 30 and 130 m above sea level:

- the shoreline of Contrada Fusco, W of the city of Syracuse at +32 m, dated by ESR at 115 ka and attributed to MIS 5.3, at ca. 100 ka;
- the Coste di Gigia, at +34 m, at the foot of Melilli, paleontologically dated by IE at  $200 \pm 40$  ka.
- The MIS 5 terrace, characterized by the fossil markers of *Strombus bubonius*, located at about +90 to +100 m in the area studied;
- the Spinagallo cave, between +120 and +130 m, on a notch of the Avola fault scarp at the intersection with the Spinagallo fault, which forms the SW border of the Florida basin. This cave is famous for its dwarf elephant remains, partly responsible for the origin of the Cyclops legend, and elephant teeth were dated by IE at  $455 \pm 90$  ka. The cave appears thus related to MIS 13 at 520 ka.

The ages of the other marine terraces are calculated by interpolation/extrapolation from this limited panel of absolute ages, whose quality and interpretation remain controversial, but whose technical assessment makes it possible to attribute a certain robustness to the age models as a whole.

For the Syracuse area, age models based on dated controls, yield by extrapolation uplift rates (in m/ka) on the order of 0.3 in the Florida Basin, 0.6 at the foot of the Monti Climiti, and 0.7 in the Augusta Basin (Catalano et al., 2010). These values are approximately doubled towards the interior of the plateau due to the eastward tilt (Pavano et al., 2022). The minimum value (0.3) is attributed to regional uplift, the rest to positive movements of fault escarpments (Bianca et al., 1999). According to these authors, these uplift rates can vary slightly depending on the assignment of terraces to a given isotopic stage, the significance of the dated material (marine vs. continental), and the specificities of the dating methods. However, they agree on the overall magnitude and on local variations (see discussions in Antonioli et al., 2006; Catalano et al., 2010; Pavano et al., 2022).

## THE STUDIED CAVES

Three caves were studied (Palombara, Scrivilleri, Monello), with entrances between 100 to 150 m above present sea level, plus one cave (Spinagallo) from which we used published data. All are located in the calcarenites and algal calcirudites of the Monti Climiti Fm., in the upper Syracuse Member (Burdigalian-Serravallian), on the horsts on either side of the Florida basin. Their main data is shown in Table 1 and their location in Figure 1.

The **Palombara Cave** (cave register no. 7001SI-SR) is accessed at an altitude of 143 m, on a marine terrace. Its age varies according to whether it is assigned to MIS 7.5 (240 ka) (Bianca et al., 1999) or MIS 9.1 (305 ka) (Catalano et al., 2010). This is the deepest cave in the Syracuse area (-80 m), with a total length of 700 m (Ruggieri et al., 2000). It mainly consists of a main passage, which branches off near the end (Fig. 2). The cave opens through a vertical collapse shaft leading to an inclined gallery, followed by a series of narrow horizontal tubes and rifts at around 100 m a.s.l., which finally open onto an internal shaft. Its sloping floor leads to the "Vase Chamber", named after a calcified ceramic, left under a gutter by Neolithic people. This chamber corresponds to the lowest point of the cave at -80 m, at the bottom of a U-loop. A slippery slide leads up, back to the horizontal level at 100 m, then to the Guano Chamber, home to a large colony of bats. From here, two horizontal branches diverge at the same altitude. Three 20-m-deep shafts open along the Geode Branch.

The **Scrivilleri Cave** (cave register no. 7003 SI-SR) is entered through an ancient artificial shaft near the homonymous Masseria (Farmhouse), at the foot of Monti Climiti horst, 152 m a.s.l. It is located on a marine abrasion platform, in the northern extension of the terrace attributed to MIS 9, with an age of around 300 ka. It develops

close to the base of the upper Syracuse Member (Fig. 1D). The entrance part has been known for ages for its initial parts. It has been considerably extended since 1992, to become the longest cave on the Hyblean Plateau, with over 2 km of length,

for a depth of 35 m (Arena et al., 2013). It is characterized by a maze pattern, dominated by long and high NW-SE and WSW-ENE fractures and connected by narrow sinuous conduits following the dip (Fig. 3).

Table 1. Location of the three studied sites and caves and other mentioned caves, with the altitude of their entrances and of horizontal drains, ages calculated from age models and dating. Speleometric data from the National Cadaster of Italian Caves [https://speleo.it/catastogrotte] and from the Sicilian Region [http://www.federazione speleologica siciliana.it/fsrs/catasto/catasto.html].

Cave / surface site	Speleological cadaster no.	Depth (m)	Length (m)	Latitude (°)	Longitude (°)	Altitude entrance (m)	Alt. main drain(s) (m)	Alt. of corresponding terrace (m)	MIS*	Age <sup>§</sup> (ka)	Age (ka)
Palombara	7001SI-SR	-80	700	37.106288	15.194233	143	100	110 (Eurialo)	7.3/7.5	240 <sup>a</sup>	>780 <sup>c</sup>
Paleo-cliff				37.106443	15.189533			≈140 (notch)	9.1	305 <sup>a</sup>	<b>603<sup>d</sup> ± 182</b>
Scrivilleri	7003SI-SR	-35	>2000	37.141278	15.159957	152	120, 140	150-160	9.1	305 <sup>a</sup>	<780 <sup>c</sup>
Spinagallo	7006SI-SR	-15	30	37.003367	15.181433	125	125	125	13	520 <sup>b</sup>	455 ± 90 <sup>b</sup>
Monello	7007SI-SR	≈ -40	200	37.017974	15.165145	100	90, 77, 60	90	9.3	330 <sup>b</sup>	<780 <sup>c</sup>
Chiusazza	7004SI-SR	≈ -15	190	37.026338	15.159486°	107	90	90	9.3	330 <sup>b</sup>	

\* Marine isotope stage; § From age model of: <sup>a</sup> Catalanò et al. (2010); <sup>b</sup> Pavano et al., 2022; <sup>c</sup> paleomagnetism (this study); <sup>d</sup> U/Th age (this study).

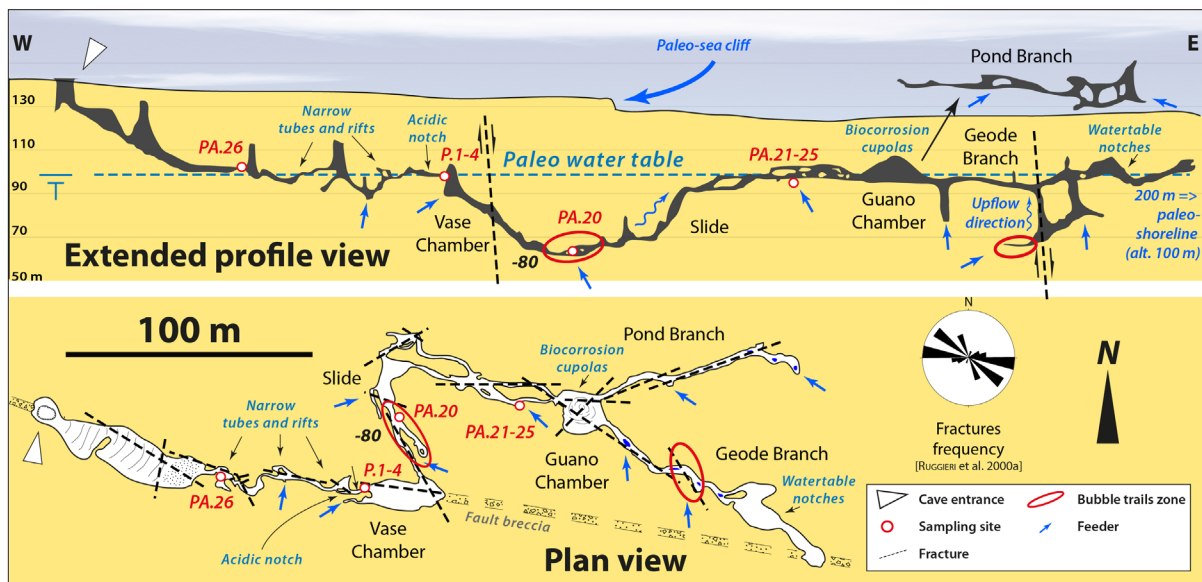


Fig. 2. Survey of Palombara Cave (redrawn after Ruggieri et al., 2000). Rose diagram, sampling sites, and hypogenic flow indicators are shown.

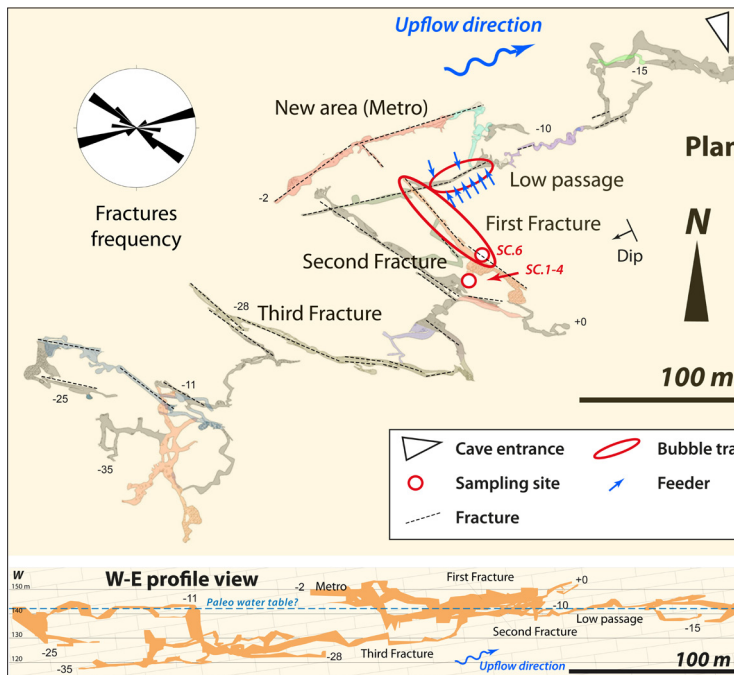


Fig. 3. Survey of Scrivilleri Cave. Plan view redrawn after Arena et al. (2013), profile courtesy of G. Spitaleri and G. Guidice. Rose diagram, sampling sites, and hypogenic flow indicators are shown.

The **Monello Cave** (cave register no. 7007 SI-SR) is entered at an altitude of 100 m a.s.l., on the southern edge of the Florida basin, close to the NW-SE Spinagallo fault escarpment, which bounds the Canicattini-Cassibile horst further south, and at the mouth of a canyon descending from the plateau. It is located on a marine abrasion platform attributed to MIS 9, with an estimated age of around 330 ka. The cave is 200 m long and around 40 m deep. It is mainly made up of horizontal passages at different altitudes, arranged as staircases (Fig. 4). The passages are widened into a room close to the entrance, followed by high and narrow passages along fractures,

before turning to a tube-like profile in the gallery at -25 m. To the South, a series of shafts along fractures

leads to the lowest point at about -40 m (Ruggieri & Amore, 2000).

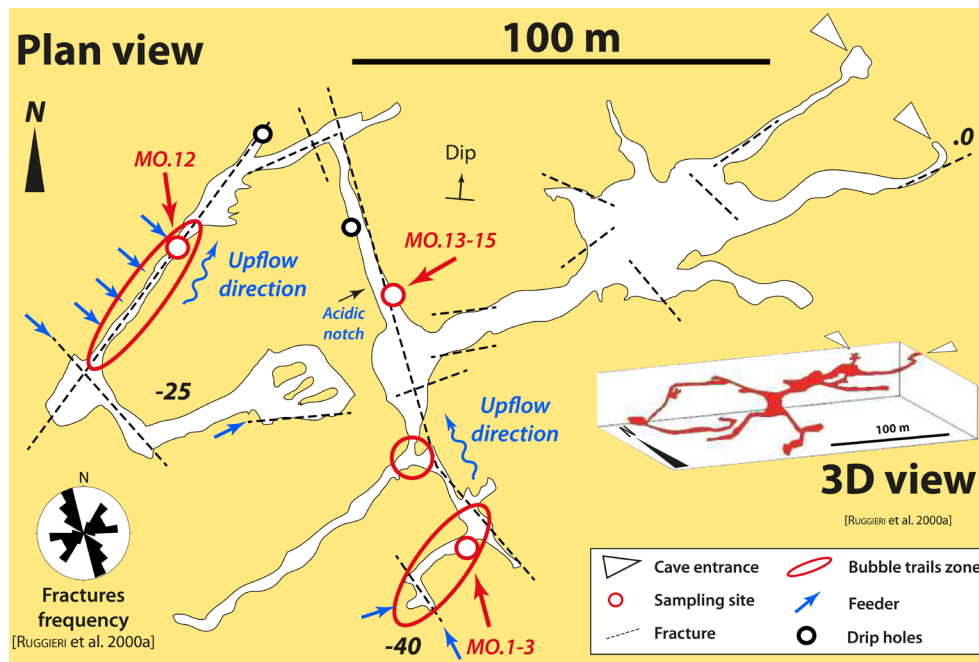


Fig. 4. Survey of Monello Cave (redrawn after Ruggieri & Amore, 2000). Rose diagram, sampling sites, and hypogenic flow indicators are shown.

## SEDIMENT PROFILES AND SAMPLES

### Palombara Cave

All sampling sites are located on Figure 2 and are described from the entrance. Analytic results are summarized in Tables 2, 3, and 4.

Sampling site PA.26 is located in a labyrinthine zone along the trend of the inclined entrance gallery. The section consists of a white layer, several cm-thick (not sampled) covered with a black layer with some thin white laminations, with bat guano sprinkled on top (Fig. 5A).

P.1-4 sampling site is located on top of the shaft opening to the Vase Chamber. It consists in a colored, laminated, fine fluvial sequence. From bottom to top, 6 levels can be visually differentiated (Fig. 5B). Bottom: grains of homogeneous light-colored sand from calcarenite bedrock disaggregation (not sampled); P.4: beige laminated clay deposit; P.3: black laminated clay deposit; P.2: whitish laminated clay deposit; P.1: orange laminated clay; P.0: old, soft guano.

Sample PA.20 is located shortly beyond the low point at -80 at the start of the climb, on the right-hand side of the wall. It is a sample of the bedrock, including bubble trails.

Sample site PA.21-25 consists of two laterally connected bodies, in the horizontal passage between the top of the Slide and the Guano Chamber (Fig. 5C). PA.21-22 is located 2 m down on the right, in a feeder, on the left wall. PA. 23-25 is located at the mouth of the feeder where it intersects the horizontal passage. There are 4 main layers of contrasting color, resting on the rocky base. From bottom to top: a laminated red clay more than 30 cm thick (PA.21-22); an aerated white sand with a few black beds (PA.24); a multicolored black-white-orange clay layer (not sampled here), very similar to P.1-4 described above; a thick, old, soft guano deposit (PA.25); a thin purple crust locally covering the edge of the old guano (PA.23). White disaggregation sand is sprinkled over everything.

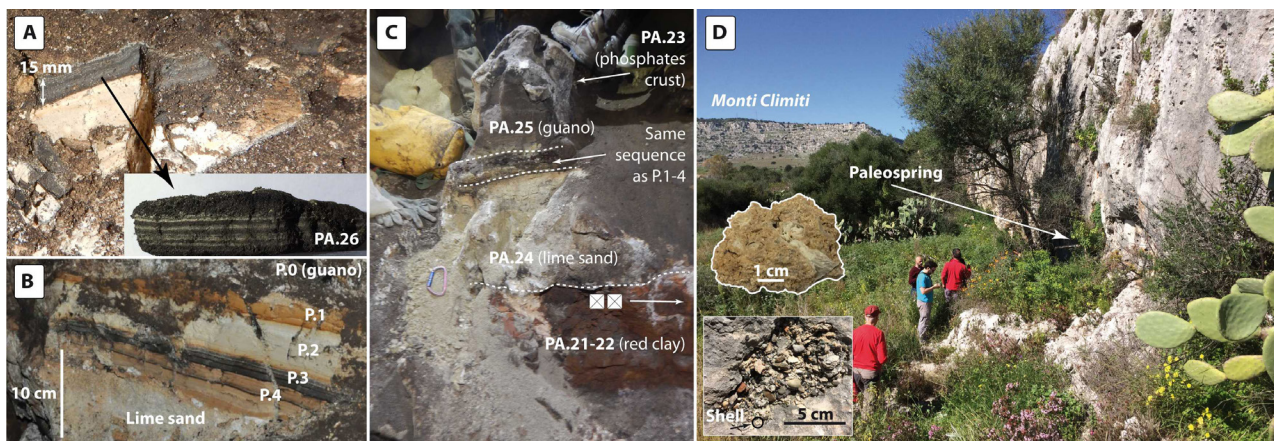


Fig. 5. Sediments in Palombara Cave, with location on Fig. 2. A) Section and sample PA.26 (photo. M. Vattano). B) Sample site P.1-4 (photo. Ph. Audra). C) Stratigraphy of sampling site for PA.21-25, the white squares indicate a possible inverse magnetic orientation (photo. M. Vattano). D) Paleocliff of MIS 7 surrounding the marine terrace of MIS 9 at Palombara located above, with Monti Climiti in the background. Insets: littoral shell deposits, consisting of carbonate sands (top) and allogenic gravels (bottom) (photo Ph. Audra).

### Palombara marine cliff

Palombara Cave is located on a promontory-shaped marine abrasion platform attributed to MIS 9, surrounded by a paleoclipf of MIS 7 (Fig. 1B). To the W, overlooking the Florida basin, the marine notch of the paleoclipf contains cemented veneers of allogenic, transported gravels and carbonate sands, both with shell debris, however without any foraminifers (Fig. 5D). A small tube-shaped conduit at the base of the notch represents an ancient littoral spring and contains limestone pebbles over 10 cm long.

### Scrivilleri Cave and Quarry

In addition to Scrivilleri Cave (samples marked SC and located on Figure 3), the nearby quarry showed evidence of karstification, with sediment-filled channels (samples marked SQ for Scrivilleri Quarry).

SC.6 is located in the First Fracture, along the left wall. It is a rock sample close to a bubble trail.

SC.1-4 is located in a deep side passage of the First Fissure chamber. This 25-cm-thick sequence rests on 3 cm of weathered rock, made of loose grains of calcarenite (not sampled) (Fig. 6A). SC1-2 is a brown laminated clay at the base of the sequence. It is covered by several layers of clay, lime sand or a mixture of

the two (not sampled). SC.4 is a thin black layer of old guano which has been altered into phosphate minerals. SC.3 is again a thick layer of lime sand. The surface is covered by a dusting of lime sand from the disintegration of the overlying wall, and guano.

A nearby quarry to the N of Scrivilleri Cave exposes karst features, mainly spongy vugs and channels filled with sediments. The S part of the quarry face is dotted with highly altered spongy voids where the walls of the conduits can be distinguished after removal of sediment consisting in thick white calcite layers interbedded in sandy-clay deposits.

SQ.1-2 is located on the N quarry face, at the foot of the first terrace (Fig. 6B). A void is filled by a layer of calcite spar (SQ.1), resting on the weathered substrate, and covered by a thick black indurated layer (SQ.2). The whole package is covered by a hardened platy lime layer (not sampled).

SQ.3-4 is located in the middle of the first quarry face, on the W side. A former conduit along a fracture is filled by a layer of brown-black clay (not sampled), topped by loose lime sands (SQ.3), then by highly indurated lime silts (SQ.4) (Fig. 6C). SQ.8 basal calcite is in the same stratigraphic position as SQ.1, filling the lower part of tubes.

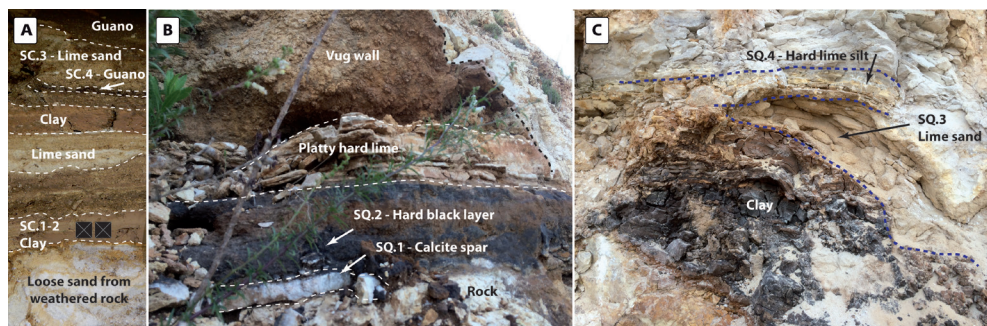


Fig. 6. Sediments in Scrivilleri Cave and Quarry. A) Stratigraphy of SC.1-4 profile, located on Figure 3. The black squares indicate a normal magnetic orientation. The view is 20 cm high (photo D. Cailhol). B) Stratigraphy of SQ.1-2 profile. The image shows a sequence approximately 20 cm thick (photo Ph. Audra). C) Stratigraphy of SQ.3-4 profile. The image shows a sequence approximately 50 cm thick (photo Ph. Audra).

### Monello Cave

The upper level of the cave contains mainly breakdowns covered with flowstone. In the entrance of the southern series, laminated lime sand about 50 cm-thick, is covered with a 30-cm-thick white calcite flowstone. In the deepest part after the shafts, when entering the gallery to the right, the MO.1-3 fluvial sequence was sampled (Fig. 7A). From the bottom to top, it consists of: loose coarse lime sand from calcarenite disaggregation (not sampled); a 5-cm-thick layer of brown plastic clay (MO.1-2); a mixture of well-

laminated clay and lime sand (not sampled); a 2-3 cm thick flowstone (not sampled); a series of laminated clays about 10 cm thick (not sampled); ending with about 5 cm of very compact lime silts (MO. 3). All these layers are finely laminated.

Various types of calcite were sampled (Fig. 7B, 7C). MO.12 is a vein of symmetric calcite from a fault on the roof of the gallery with numerous feeders. MO.13 is flowstone covered with lime sand, and brown clay or guano. MO.15 is a calcite vein on the wall from the first room, close to the path.

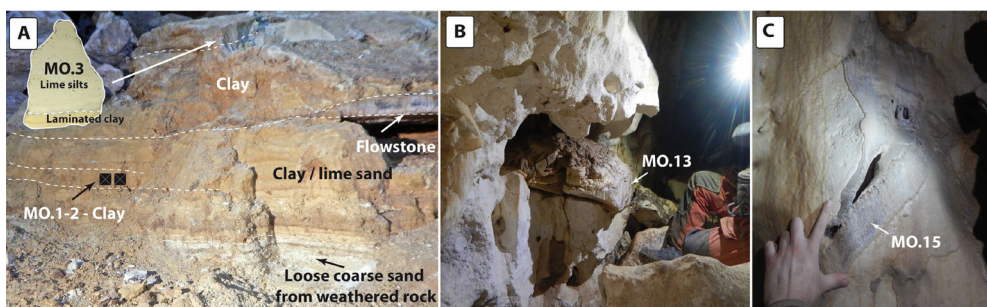


Fig. 7. Sediments in Monello Cave, with location on Figure 4. A) Stratigraphy of MO.1-3 profile. The image shows a sequence approximately 50 cm thick. The black squares indicate a normal magnetic orientation (photo D. Cailhol). B) MO.13 flowstone covered with lime sand and brown material (clay or guano) (photo M. Vattano). C) MO.15 symmetric calcite vein cut by the cave passage (photo M. Vattano).



## METHODS

Cave sediments were sampled for mineralogical analysis. Samples were analyzed by X-ray powder diffraction (XRPD) on a Philips diffractometer (40 kV and 20 mA, CoK $\alpha$  radiation, Graphite filter) at the CEREGE – CNRS, Aix-Marseille University, France. Carbonate content was calculated by decarbonation after HCl treatment. A carbonate sandy deposit attached to the coastal notch of the Palombara marine terrace was sampled for U/Th dating at the Institute for Global Environmental Change, University of Xi'an Jiaotong, China. Activity ratios were determined using a NU Plasma MC-ICP-MS following the procedure of Cheng et al. (2013). For paleomagnetism of clastic sediments, the magnetic remanence was investigated with alternating field (AF) demagnetization in the paleomagnetic laboratory at the University of Montpellier, France (for details see Montheil et al., 2023). Measurements of carbon and oxygen stable isotope composition of carbonates were carried out at the University of Cambridge, UK (for details see Gázquez et al., 2018) and at the Institute for Nuclear Research (ATOMKI) in Debrecen, Hungary. The analyses at ATOMKI were done on an automated GASEBENCH II sample preparation device attached to a Thermo Finnigan DeltaPLUS XP isotope ratio mass spectrometer. The results are reported as  $\delta^{13}\text{C}$  and  $\delta^{18}\text{O}$  values relative to Vienna Pee-Dee Belemnite (VPDB). Analytical precision was  $\pm 0.08\text{‰}$  for both.

## RESULTS

### Microscopic description

Lime sands were examined under an optical microscope and compared with the host calcarenite. The Monti Climiti calcarenite (PA20) was sampled along the cave wall. It is a grain-supported calcarenite with foraminifers, echinoderms, and bryozoans allochems. The outer surface shows corrosion of the small crystals of the matrix, leaving coarse grains in relief. All lime sands are almost exclusively composed of carbonates (from 93 to more than 99%) (Table 2). They are made of coarse grains of transparent calcite (SQ.3 = 200–500  $\mu\text{m}$ ; SQ. 4 = 100–300  $\mu\text{m}$ ), with angular clasts (SC.3, SQ.4, MO.3). In these coarse samples, we systematically find stalks of crinoids (SC.3, PA.24, Fig. 8). These two samples do not show any layered structure, the grains have not been transported. Other samples of finer grain size (SQ.4) may show slight rounding of the grains (SQ.3) and clear lamination (SQ.4), resulting from a very short transport before deposition. Sample MO.3 has the finest particle size (5  $\mu\text{m}$ ) corresponding to sorting then deposition by very slow flows, such as in decantation basins or overbank deposits. The samples that are not completely composed of carbonates (SC.3) are accompanied by a minor detrital assemblage (clay, Fe oxides, quartz, feldspars, etc.). SC.3 also shows an alteration, with corrosion of the grains in the form of sharpened edges of crystals and corrosion pits. Some grains are covered with a thin brown coating, probably Fe oxides.

The hard black layer of the Scrivilleri Quarry pockets (SQ.2) consists of a fine black matrix. Hollow crinoid tubes can also be observed (300  $\mu\text{m}$ –2 mm), coated by secondary calcite crystals that appear in relief, together with fibrous filaments (some  $\mu\text{m}$ , up to 50  $\mu\text{m}$ ).

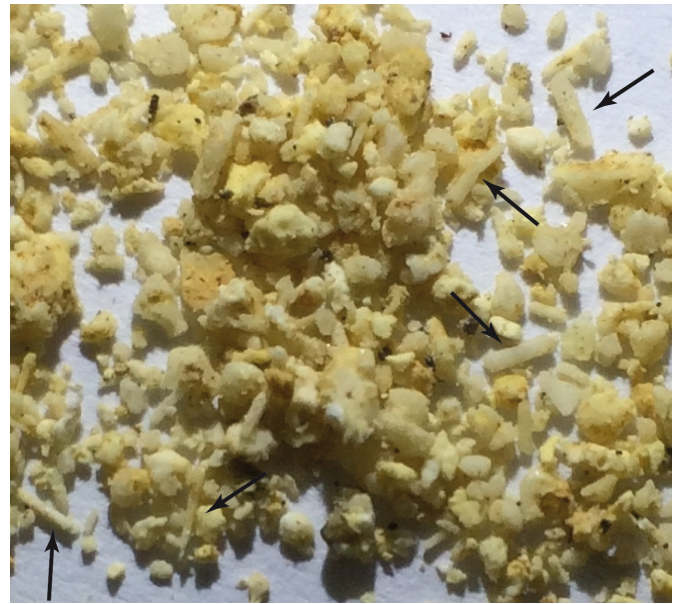


Fig. 8. Lime sand. Angular calcite grains resulting from disaggregation of the calcarenite walls through condensation-corrosion processes (PA.24 sample). Crinoid bioclasts are indicated by arrows. Black dots are bat guano particles. The image is 3 cm wide.

### Mineralogical determination by XRPD

The results of mineralogical analysis by X-ray powder diffraction (XRPD) are summarized in Table 2. Several samples contain phosphates derived from the mineralization of bat guano. Common phosphates such as hydroxylapatite and fluorapatite result from interaction with the carbonate host rock. Taranakite, a potassium-aluminum phosphate found at Palombara, results from the reaction between acidic guano leachates and allogenic clastic sediments, notably clay (Audra et al., 2019). Robertsite is a manganese phosphate. Mn is present also in Palombara as an oxide, todorokite. The goethite present at Scrivilleri also results from the alteration of clastic sediments by acid guano leachates.

The second group of minerals is of clastic origin, with quartz, mica (muscovite) and titanium oxide (anatase). These minerals are not present in the host rock, and come from allogenic contributions carried into caves by runoff and deposited by decantation in the form of fine laminated sediments. Clays such as kaolinite and montmorillonite are partly derived from the alteration of these fluvial sediments by guano-derived acids (Audra et al., 2021).

### Radiometric dating of calcite (U/Th)

The U/Th-dated calcitic sandy deposit of the coastal notch younger than the Palombara marine terrace yielded an age of  $603 \pm 182$  ka, i.e., between 785 and 421 ka (close to secular equilibrium). The carbonate sand had a high  $^{238}\text{U}$  concentration (1.3 ppm), the  $^{230}\text{Th}/^{232}\text{Th}$  atomic ratio suggests some detrital contamination (Supplementary Table S1). The age can be considered a

good estimate, however, the margin of error of ca. 180 ka remains relatively large. Consequently, considering that these marine terraces have to be attributed to

high relative sea levels prior to MIS 11. The Palombara terrace at the top of the cliff would correspond to an older stage, such as MIS 15 (621-563 ka) or older.

Table 2. Mineralogical composition of cave sediments. (\*) published in Audra et al. (2019).

Sample no.	Cave	Observation	CaCO <sub>3</sub> (%)	XRPD
SC.3	Scrivilleri	Weathering sand on top	93	Goethite, kaolinite, anatase, quartz, montmorillonite, muscovite
SC.4 *		Black guano layer		Calcite, carbonate fluorapatite, kaolinite, quartz, goethite
SQ.2	Scrivilleri Quarry	Fe-Ox	Strong effervescence with HCl	Quartz, goethite
SQ.3		Carbonate sand	97.5	
SQ.4		Fine hardened silt	>99	No residue
P.1	Palombara	Irregular yellowish laminae		Kaolinite, quartz
P.2		Thin dark yellow laminae		Kaolinite, quartz
P.3		Grey laminae (some on yellow material)		Quartz, kaolinite
P.4		Thin light hazel laminae		Quartz, kaolinite
PA.23 *		Violet crust, phosphate		Hydroxylapatite, robertsite
PA.24		White carbonate sand	>99	
PA.26		Black laminae		Calcite, kaolinite, todorokite
MO.3	Monello	White compact "clay" on top	>99	

### Paleomagnetism of fluvial deposits

Paleomagnetism was measured for decanted clay layers located at the base of the fluvial sequences of the 3 studied caves, namely SC.1-2 (Scrivilleri), PA.21-22 (Palombara), and MO.1-2 (Monello). The most diagnostic Zijderveld diagrams are shown in Figure 9, all diagrams are reported in the supplementary material ([Supplementary Figs. S1-S4](#)). The interpreted chronology is shown in Table 3. SC.1-2 displays a remagnetization of undetermined origin, possibly an Isothermal Remanent Magnetization (IRM) due to sampling or storage, but with

a primary component of stable normal polarity. Polarity is definitely normal, therefore the sample is younger than 780 ka. PA.21-22 displays a strong remagnetization in the normal field, and a component of reverse polarity at very low intensity appears at the end of demagnetization. The polarity at the time of deposition is inverse, i.e. older than 780 ka, unless it corresponds to one of the geomagnetic excursions during the Brunhes Chron. MO.1-2 displays a weakly magnetized, normal primary component, showing a normal polarity, and should therefore be younger than 780 ka.

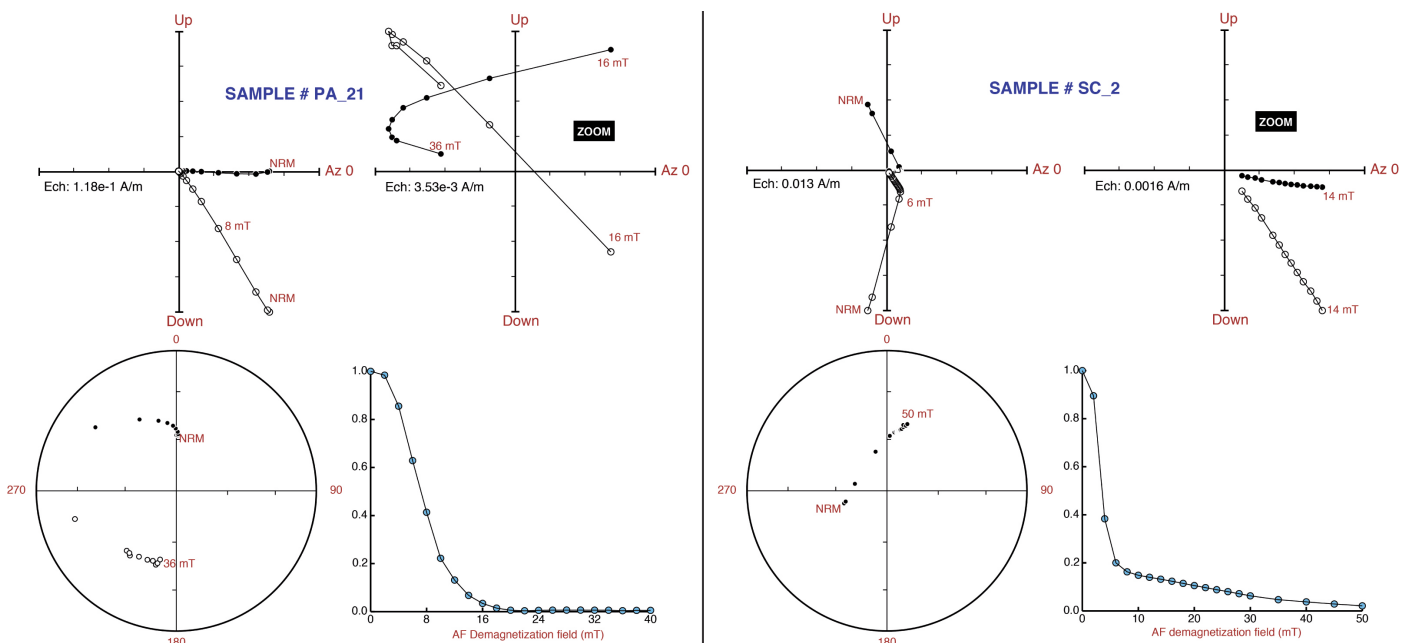


Fig. 9. Zijderveld diagrams of an inverse sample (PA.21) and a normal sample (SC.2). All diagrams can be viewed in the Supplementary Fig. S1.

Table 3. Paleomagnetic polarity interpretation.

Sample no.	Altitude (m)	Polarity	Age estimate (ka)
SC.1-2	≈125 m	NORMAL	<780
PA.21-22	100 m	probably INVERSE	>780
MO.1-2	≈70 m	probably NORMAL	<780

### Carbonate stable isotopes

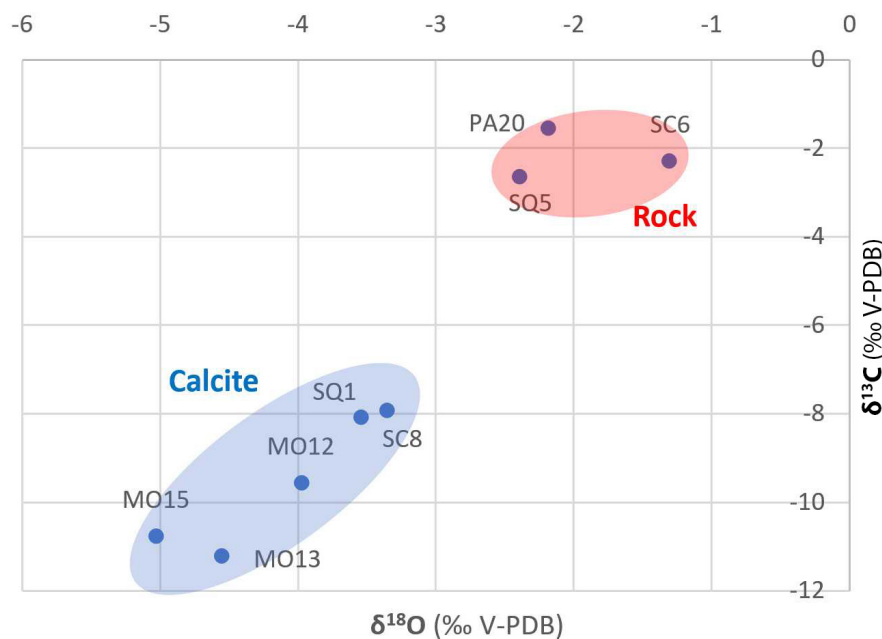
Carbon and oxygen stable isotopes have been measured on the following samples: calcite fibers along a fault (MO.12), calcite in a vein (MO.15), speleothems (SQ.1, MO13) and host rock (SC.6, SQ.5, PA.20). The results

are summarized in Table 4 and plotted in Figure 10.

The secondary calcite samples have distinctively lower  $\delta^{13}\text{C}$  and  $\delta^{18}\text{O}$  values (-11.2 to -7.9‰ and -5.0 to -3.4‰, respectively) compared to the calcarenite bedrock (-2.7 to 1.5‰ and -2.4 to 1.3‰, respectively).

Table 4. Stable isotopes of carbonates (rock and calcite speleothems).

Sample no.	Cave / Location	Material	Sample code (Lab)	$\delta^{13}\text{C}$	$\delta^{18}\text{O}$
				‰ (V-PDB)	
SC.6	Scrivilleri	Calcarenite (bedrock)		-2.3	-1.3
SQ.1	Scrivilleri Quarry	Thick basal calcite spar		-8.1	-3.5
SQ.5		Calcarenite (bedrock)	SC12	-2.7	-2.4
SQ.8		Calcite flowstone	SC11	-7.9	-3.4
PA.20	Palombara	Calcarenite (bedrock)	PA20 (n = 10)	-1.5	-2.2
MO.12	Monello	Fault calcite	SC8	-9.6	-4.0
MO.13		Calcite crust	SC9	-11.2	-4.6
MO.15		Calcite vein	SC10	-10.8	-5.0

Fig. 10. Isotopic crossplot ( $\delta^{18}\text{O}$  vs.  $\delta^{13}\text{C}$  values) of carbonate host rock and calcite speleothems.

### Cave patterns

Plan views do not show the typical dendritic patterns corresponding to epigenic caves, with a downstream convergence of tributaries toward a main drain (Audra & Palmer, 2013). This might also be due to an explorational bias, but recent speleological activity in all three caves, and our own fieldwork, do indicate that most explorable cave passages have indeed been surveyed. In contrast, Palombara main drain diverges downstream (Fig. 2), Monello subdivides downstream into three branches (Fig. 4), and Scrivilleri develops into a labyrinth (Fig. 3). These patterns are clearly

constrained by local fracturing (Ruggieri & Amore, 2000; Ruggieri et al., 2000): the faults bordering the Monti Climiti, the Florida basin, and the Spinagallo and Avola faults, for Scrivilleri, Palombara, and Monello, respectively (Fig. 1C). At the scale of the networks, dip has generally very little influence, with the exception of short segments of conduits. In Scrivilleri however, part of the cave pattern is controlled by bedding planes (Fig. 3).

In profile, the patterns are organized in horizontal segments connected by inclined or subvertical segments. These horizontal segments cannot be

considered as stages marking distinct speleogenetic phases, as they are linked by the non-horizontal segments, with apparent morphological continuity, such as in Monello. Although successive phases are probable (i.e. oscillating sea level), on the whole the patterns can be considered monogenetic, with only subsequent local phases of adjustment (collapses, sedimentation, etc.) leaving the general organization. Horizontal levels can only be considered as privileged flow zones within a given altitudinal range (Table 1). Only Palombara has an undeniable horizontal level 40 m below the surface at an altitude of 100 m, marked by a series of characteristic notches (see below); the entrance zone results from collapses connecting at depth to the main drain, while the loop at -80 corresponds to a deep passage in the phreatic zone, with the descending shafts also connected to this horizontal level. In addition, Scrivilleri pattern seems to be partly controlled by a tier at about 140

m a.s.l. (Fig. 3). However, its complex maze pattern probably includes other types of control that remain to be investigated.

### Speleogens

Speleogens are the features produced by dissolution of the host rock, which are characteristic of their environment, especially the type of flow. In this study this mainly includes rising flow and late stage (bio) condensation-corrosion.

Recharge features (feeders), visible as small subvertical conduits, impenetrable at close range, are evidence of rather short but clearly ascending flows. They are grouped in series (Figs. 2–4), generally on one side of a fault-aligned gallery (Scrivilleri, Monello), at the base of a series of shafts (Palombara, Monello), extended into a ceiling channel (Scrivilleri) or in a chimney (Palombara), forming a typical Morphologic Suite of Rising Flow (MSRF; Klimchouk, 2007) (Fig. 11).

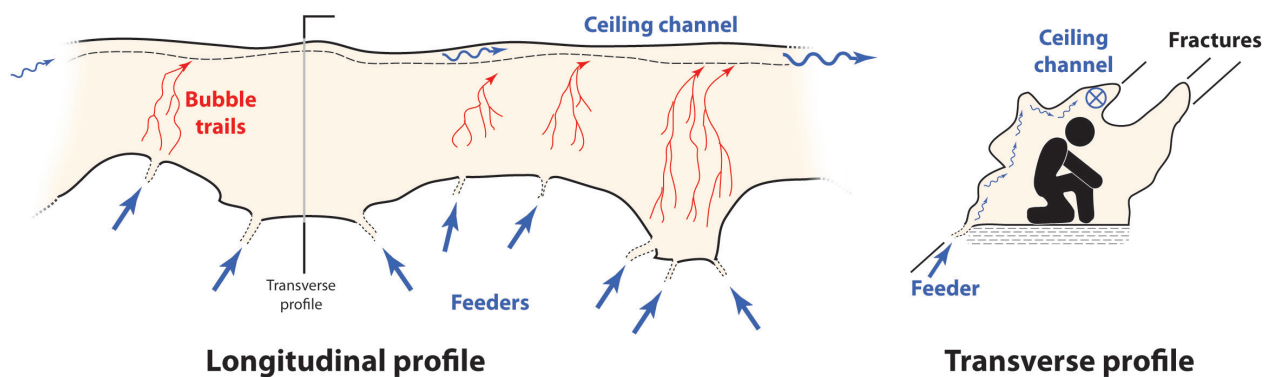


Fig. 11. Morphologic Suite of Rising Flow (MSRF) showing flow rising from depth from tiny feeders and converging toward a ceiling channel, whereas bubble trails form as the deep-seated water rises and loses  $\text{CO}_2$  (see Monello and Scrivilleri caves).

Bubble trails refer to rising solutional grooves developed on overhanging walls and caused by corrosive fluids or  $\text{CO}_2$  degassing bubbles under phreatic conditions as a result of a drop in pressure during the rise of deep-seated water carrying carbon dioxide in solution (Chiesa & Forti, 1987). They are typical of hypogenic caves (Audra et al., 2009a and references therein; López-Martínez et al., 2020). Bubble trails are present in all the studied caves, in deep zones near feeders or

along major fractures (Figs. 2–4). These rising channels converge upwards in branching structures of increasing size, passing to ceiling channels, then to ceiling cupolas where the gas accumulates. They appear in the wall, in massive, unfractured rock (Figs. 11, 12). These morphologies resulting from carbonic degassing from the rock mass, typical of porous rocks, have also been mentioned in caves in Miocene calcarenites on the Mallorca Island in Spain (Fornós et al., 2011).

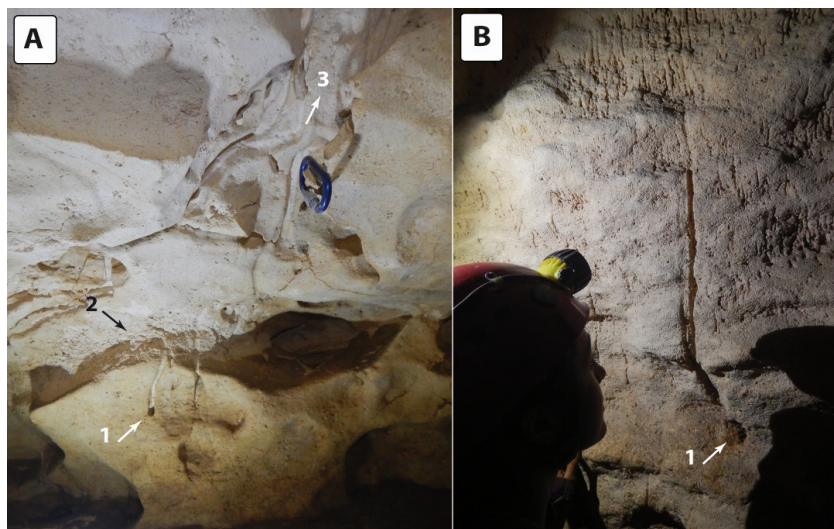


Fig. 12. A) Bubble trails from Monello Cave emerging from porous rock (1), leading to diffuse corrosion of the overhanging wall (2) and merging upward (3). B) Dense bubble trails emerging from porosity in First fracture wall in Scrivilleri Cave; the largest one emerges from a small hole (1) (Photo. M. Vattano).

When corrosion is renewed by significant aggressive input, such as sulfuric or carbonic acid, cave pools remain extremely corrosive. The aggressive water body causes lateral corrosion, which is visible as a notch with a flat top, corresponding to the surface of the pool (Audra et al., 2009b). These acid notches are different from watertable notches developed along calm rivers where small oscillations of the water table create half-elliptical cross-sections. Acid notches are present in Monello, on a block detached from the ceiling (Figs. 4, 13), and in Palombara, in a side passage above the Vase Chamber shaft (Fig. 2). Both record the corresponding altitudes of the water table, at around 90 m and 100 m, respectively. The latter corresponds exactly to the horizontal level along which Palombara Cave extends.

After drainage, the caves changed from a phreatic to vadose (atmospheric environment). Speleothem

deposition started, however few modifications occurred with original morphologies generally preserved, except in areas subject to biocorrosion. This in turn started when caves opened to the surface, allowing large bat colonies to enter. Consequently, all caves show clear signs of late-stage condensation-corrosion and biocorrosion features.

Small pockets associated with the initial phreatic stage develop perpendicular to the walls, following the fracturing, if any (Fig. 14). In contrast, biocorrosion cupolas, linked to the condensation-corrosion process due to air circulation and the presence of bat colonies, develop vertically upwards, independent of the fractures, in the form of hemispherical domes or cylindrical bell holes (Audra et al., 2016, 2017; Barriquand et al., 2021). These bat-mediated features overprint earlier cupolas and pockets of phreatic origin.



Fig. 13. Notch with flat roof formed above a corrosive pool, Monello Cave. The block detached from the ceiling has slightly rotated and tilted the notch, which is no longer perfectly horizontal. Bubble trails, developing perpendicular to and above the notch, correspond to a previous phase with higher water table. The brown deposits are recent apatite crusts resulting from bat guano mineralization (photo D. Cailhol).



Fig. 14. Ceiling pockets. A) Phreatic pockets from initial phase in Monello Cave, smaller in size and with main axis roughly perpendicular to the walls, i.e. not vertical. B) Late stage biogenic cupola in Guano Chamber, Palombara Cave. Condensation-corrosion process associated with the presence of a large bat colony creates vertical upward development of large cupolas. Note large guano heap below the cupola (photos M. Vattano).

In Palombara Cave, several chambers host bat colonies, which are responsible at least for the vertical development of large cupolas (see above) (Fig. 15). In the last chamber, remnants of a series of water-table notches and proto-conduits are visible on the walls of a dome-chamber. They are located at 100 m a.s.l., at the same altitude as the acidic notch with the flat ceiling above the Vase Chamber in the same cave (see Fig. 2). However, the notches and proto-conduits in this last chamber have been cut and smoothed by condensation-corrosion due to the presence of a bat colony and a large guano pile. The chamber has been extended upwards to form a condensation dome, and laterally expanded by biocorrosion.

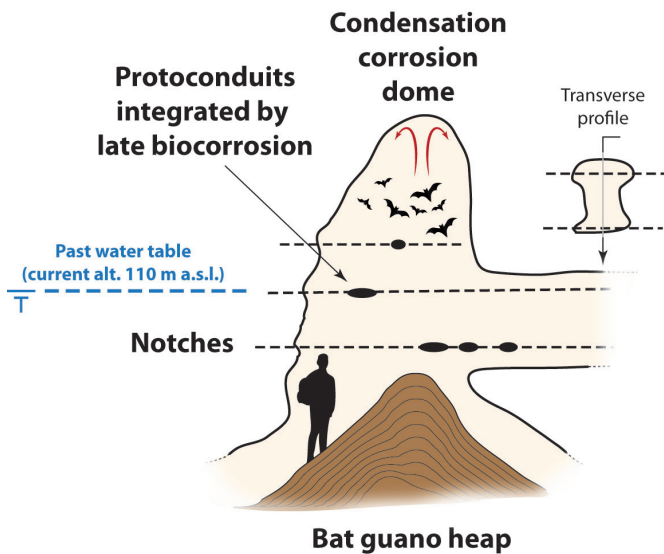


Fig. 15. Acid notches and protoconduits in Palombara Cave. Due to the presence of bat colonies the chamber expanded by biocorrosion, integrated the proto-conduits, and smoothed the notches.

Condensation-corrosion processes, amplified by the presence of bats exhaling vapor and  $\text{CO}_2$ , and by the mineralization of guano, produce locally pronounced wall alterations (Barriquand et al., 2021). In Palombara, walls subjected to biocorrosion have retreated in some places by several centimeters, as shown by the insoluble phosphate crusts remaining in place. Angular blocks of a scree have been completely

rounded by aggressive convections (Audra et al., 2016, 2017). Close to Monello, speleothems in Chiusazza Cave were heavily planed, intersecting growth laminae.

In this environment of soft calcarenites, the intergranular cement is easily dissolved, leading to the detachment of large calcite grains and the progressive disaggregation of the walls (Zupan-Hajna, 2003). The particles accumulate in deposits several centimeters thick, at the foot of the walls forming loose heaps (samples PA.24, base of profiles SC.1-4 and MO.1-3), or are reworked by local flows and accumulated in laminated deposits of more or less fine material, depending on the sorting carried out during transport (samples SC.3, SQ.3-4, MO.3). These deposits are given the name "lime sands" in this publication (Figs. 5B, 5C, 6-8).

Condensation water seeping down the ceiling is concentrated in drips from pendants. In the presence of bat colonies, the atmosphere is relatively concentrated in  $\text{CO}_2$  and  $\text{H}_2\text{S}$  and condensation moisture may become highly corrosive. Acidic percolation literally drills the rocky ground and boulders with drip holes a few centimeters wide, but several tens of centimeters deep. The walls of these drip holes are smooth or corroded, perfectly cylindrical, tapering slightly downwards into an inverted cone. They illustrate the power of corrosive substances derived from guano (Audra et al., 2016), as do the drip holes of active hypogenic caves produced in ultra-acidic atmospheres derived from  $\text{CO}_2$  or  $\text{H}_2\text{S}$  emanations (Plan et al., 2012; De Waele et al., 2016). In Monello, two main sites show a large density of drip holes (Figs. 4, 16, 17). The speleothems are cut, indicating a major change from oversaturation to aggressivity in the dripping water. Although the  $\text{CO}_2$  concentration in the atmosphere, measured during our surveys (March 2017), was only 4,300 ppm (i.e. 0.4%), and we have no chemical data on today's drip water, we do believe the formation of these drip holes might possibly be linked to a "recent" installation of the bat colony following the opening of the cave to the outside. When acid percolation hits a subvertical wall, it corrodes a half-cylinder, here, 3-4 cm in diameter (Fig. 17B).

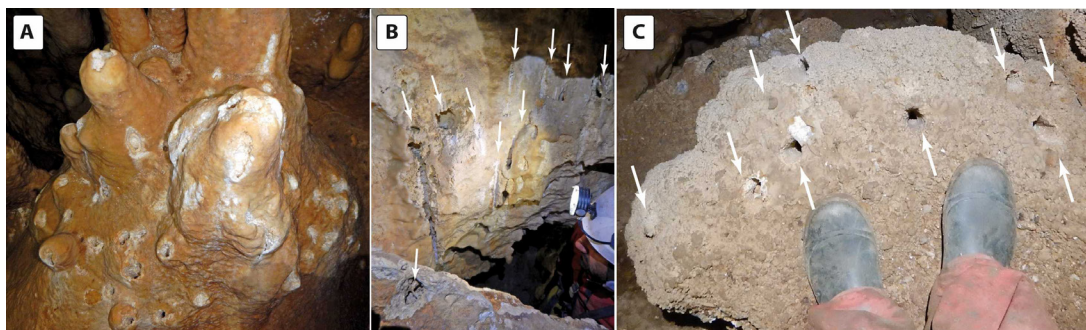


Fig. 16. Drip holes in Monello Cave actively developing through acid dripping due to the presence of bats. A) change in the chemistry of the dripping water, which became extremely corrosive and cuts a stalagmite dome. B) When the dripping water hits a subvertical wall, it corrodes half-cylinders. C) The drip holes at the foot of the person are 70 cm deep and pierce the entire limestone boulder (photos D. Cailhol (A-B), M. Vattano (C)).

The upper part of the drip holes is jagged, while the lower part is relatively smooth. When the bottom is occupied by water, it is shaped like a smooth hemispherical bowl. All indications confirm that they are actively forming. Presently, the surface above the cave is covered with a rather disturbed Mediterranean

scrubland vegetation, and soils are very thin, making present soil-derived acidity a minor contribution to drip water chemistry. Based on a lake record from SW Sicily, the climate in Sicily has been very dry during the Early Holocene (until 10,300 yr BP), a little bit wetter (but with a prominent dry period between 8,300-7,000

yr BP) in the period 10,300-4,500 yr BP, becoming as it is today (arid) since 4,500 yr BP (Magny et al., 2011). Also the stalagmite record of Carburangeli Cave near Palermo indicates the Late Holocene onset of arid conditions similar to today's (Frisia et al., 2006). The lake record of Pergusa (Central Sicily) also shows an opening of the forests starting around 5,400 yr BP,

mainly induced by climate change, and later (since 3,200 yr BP) exacerbated by human-induced land-use changes (with the increase in olive trees) (Sadori et al., 2013). The same decrease in forest cover was also seen in a marine core taken south of the Hyblean Plateau (Michelangeli et al., 2022). The density and depth of these drip holes make Monello an exceptional cave.

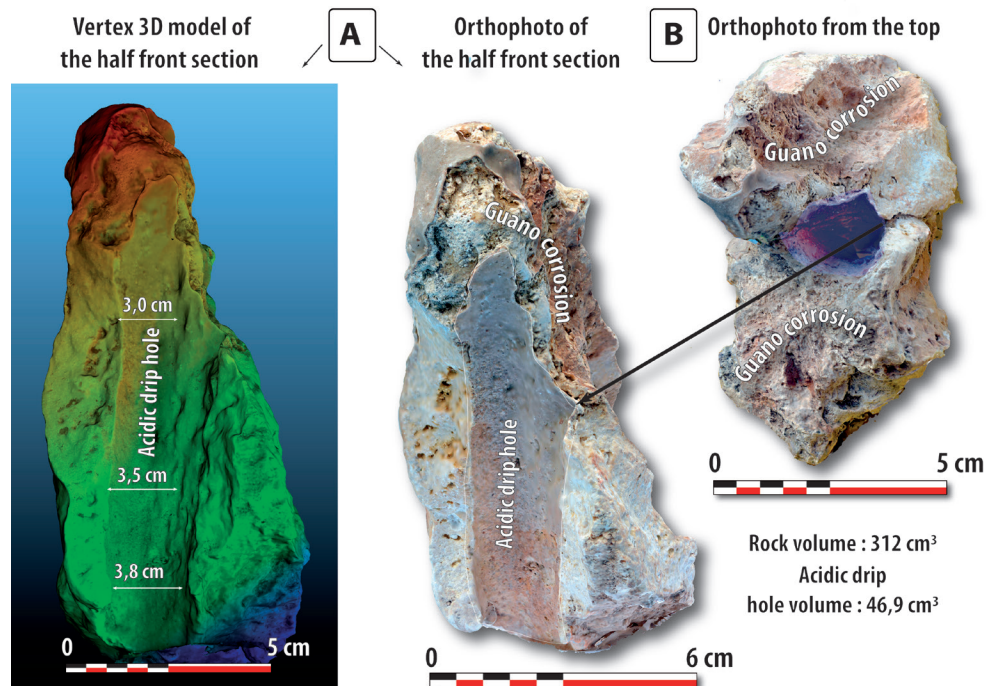


Fig. 17. Fragment of rock pierced by an acidic drip hole. A) lateral view of the sample cut vertically showing half of the cylindrical drip hole, 3-4 cm in diameter. B) View from above. The 3D model can be viewed at <https://skfb.ly/oUKHD>

## DISCUSSION

### Cave sediments

Sedimentological and mineralogical analyses revealed four types of sediment filling the caves.

Hypogenic sediments are not common. At most, the basal level of calcite spar from Scrivilleri Quarry (SQ.1), overlain by a compact ferruginous level, might be considered hypogenic. The Monello calcite vein (MO.13) could also represent an initial hypogenic stage. Isotopic analyses did not show any specific signature, indicated the spar is similar to recent meteoric speleothems. The ferruginous layer of Scrivilleri Quarry (SQ.2) could also be a precipitate resulting from the oxidation of deep waters initially loaded with reduced iron. The manganese detected could also be associated with the same origin.

Detrital allogenic sediments are derived from the surface, have been transported underground by disperse infiltration routes, and have accumulated at low levels by settling down as finely laminated clay layers interbedded with lime sands (profiles P.1-4, PA.21-22, SC.1-2, SC.3, clay below SQ.3-4, MO.1-2). The mineralogy of profile P.1-4 consists mainly of quartz and kaolinite. Kaolinite may be detrital and surface-derived like quartz, but may possibly be a secondary mineral resulting from in-situ alteration of detrital deposits under the influence of soil acidification during guano mineralization, as observed where these detrital-guano associations exist (Audra et al., 2021, 2023).

The sediments weather in situ by physical and biogenic processes. Lime sands come from the weathering of soft calcarenite walls, producing a residue of the bedrock, as attested by fragments of marine fossils and coarse calcite grains derived from the disaggregation of the walls. They result from differential corrosion of the walls, dissolving the carbonate cement and releasing the coarse calcite grains, which break away by gravity and accumulate at the foot of the walls. This process is clearly active at many sites, where accumulations of fine carbonates are present at the foot of the walls and cover recent bat guano. The disintegration proceeds in atmospheric (dewatered) environments, due to condensation, linked to air exchanges with the surface and is considerably increased by the presence of bat colonies. In the latter case, condensation-corrosion is referred to as biocorrosion (Barriquand et al., 2021). Part of these lime sands has remained intact without reworking, producing porous, aerated, and unconsolidated deposits (base of profiles P.4, SC.1-2 and MO.1-2, PA.24). Another part has been reworked by vadose runoff, sorted, and deposited as bedded accumulations of compact silts interbedded with clay deposits (SC.3, SQ. 3-4, consolidated deposits overlying SQ.2, MO.3). They make up a significant proportion of the clastic deposits observed in the studied caves. Opening of these caves to the surface has probably occurred rather recently (some tens to little over 100 ka), as the fresh nature of the weathered host rock

appears to indicate. Secondary cave minerals result from the weathering of the carbonate bedrock or of detrital allochthonous sediments, particularly under the influence of acidic leachates produced by the decay of bat guano (Audra et al., 2019). Phosphates, such as hydroxylapatite and fluorapatite, result from the interaction between guano and the carbonate bedrock (SC.4, PA.23). Robertsite, a manganese phosphate (PA.23), and todorokite, a manganese oxide (PA.26), could result from the concentration of metals along redox boundaries via the metabolism of fungi involved in guano mineralization under anaerobic conditions (Burford et al., 2003). The source of Mn can be related to either surface soils or diffuse input of hypogenic fluids. Clays such as kaolinite (SC.3-4, P.1-4, PA.26) and montmorillonite (SC.3), associated with phosphates and weathered detrital deposits, are most likely part of such weathering processes through guano leachates.

### The age of the marine terraces and the corresponding caves studied

Assigning an age to a given cave using marine terraces is a complex issue, requiring assessment of the following chronological arguments: the accuracy of the marine terrace age in which it develops; the relationship between the cave (its main drain) and its morphological environment (the marine terrace); the accuracy of cave dating; and the chronological significance of dated objects in relation to the main period of activity of the cave in question.

The marine terraces dated in the Palombara tectonic compartment are the ones at +32 m at Contrada Fusco near Syracuse and at +60 m at Belvedere, whose ages obtained by ESR are estimated at 80-100 ka and 120-143 ka, respectively, which would give an uplift rate of about 0.65 m/ka (not considering the probably rather slow (<0.1 mm/a) denudation rate of the terraces in the study area, which would lower these uplift rates). In fact, the age of the Palombara terrace at +150-160 m would be as old as 230-245 ka. With a lower uplift rate of 0.53 m/ka (Catalano et al., 2010), its age would be older, about 305-330 ka. Scrivilleri is located 5 km NW of Palombara at a similar altitude and possibly on a contemporary terrace. The Palombara Cave notches, located at 100 m a.s.l., would thus have an age of about 210 ka. Similarly, the Scrivilleri tiers, at 140 and 120 m a.s.l. would range in age between 265 and 225 ka.

For Monello Cave, located in another tectonic compartment, the marine notch close to Spinagallo Cave at +120-130 m is dated using paleontological remains by IE at 455 ka, and the corresponding marine level would be that of MIS 13 at 520 ka. Monello Cave, opening at a lower altitude, around +100 m and associated with the +90 m terrace, would therefore correspond to MIS 9.3 at 330 ka (Pavano et al., 2022). In short, based on the chronologies obtained from the marine terraces, Palombara would be approximately 210 ka old, Scrivilleri 225-265 ka, and Monello 330 ka.

However, from marine sediments from the Palombara marine notch at +140 m a.s.l., we obtained a radiometric age of  $603 \pm 182$  ka (note the large uncertainty), i.e. older than the expected

age calculated from the terraces. Moreover, in the Palombara Cave, some sediments have shown reverse magnetic orientations, so are most probably >780 ka.

These apparent contradictions show that several hypotheses can be considered, alone or in combination:

- marine sands dated by U/Th could rework older carbonate sand grains, whose mean age would not be significant;

- the paleomagnetic inversion could correspond to a younger geomagnetic incursion during the Brunhes Chron, and the Palombara sediment deposit would therefore be <780 ka. However, such situation has a low probability;

- In the Palombara compartment, the marine terraces are dated from a few points around +30 m a.s.l., and by the *Strombus bubonius* benchmark of MIS 5 located around +90 m. Clearly, extrapolations to higher and older terraces must be treated with caution;

- dating contains uncertainties. For example ESR on marine terraces is linked to the determination of the equivalent and the annual dose. For AAR on paleontological remains, the age depends on temperature and water content history, and recent microbiological processes may introduce "fresh" amino acids. Such method of dating is no longer used outside cold zones (Pitman, 2010; Powel et al., 2013). Whatever the quality of the analytical protocol and the environment considered, the error bars may be greater than given, and the ages always remain debatable;

- finally, it may be possible that the caves have developed mainly during the glacial low-stands, when the climate in these southern Mediterranean regions was wetter (Columbu et al., 2020); in that case, the marine terraces would contain older cavities.

We do not pretend to question the chronologies acquired previously and by other methods, we simply point out that their use, by extrapolation to higher and older terraces, is not very reliable, and that the age of the caves contained in these terraces could be older than a simple age/altitude model would suggest.

### Speleothem isotopes

The secondary calcite samples have distinctively lower  $\delta^{13}\text{C}$  and  $\delta^{18}\text{O}$  values compared to the calcarenite bedrock. Their relatively low  $\delta^{13}\text{C}$  values indicate organic sourced carbon. Assuming they formed under isotopic equilibrium, we can estimate the formation temperature from their carbonate  $\delta^{18}\text{O}$  values, and using  $-5.5 \pm 1.0\text{‰}$   $\delta^{18}\text{O}_{\text{VSMOW}}$  values for the paleowater, based on the isotope composition of modern groundwater in the region (Schiavo et al., 2009). Using the formula of Daëron et al. (2019), the estimated formation temperatures range between 7 and 24°C, and indicate that the speleothems formed at relatively normal (i.e., mean annual surface) temperatures, without a significant hydrothermal component. At Scrivilleri Quarry, the calcite spar SQ.1 has an almost identical isotopic composition to the calcite flowstone, suggesting formation from fluids with similar composition. Nevertheless, the stratigraphy at SQ.1, which is below a thick iron oxide layer, may indicate a phreatic origin, possibly related



to the earlier speleogenetic phases. The samples from Monello Cave (MO.12, 13,15) have a somewhat lighter isotopic composition. Their  $\delta^{18}\text{O}$  values (-4.0 to -5.0‰) might reflect somewhat higher temperature or lower paleofluid  $\delta^{18}\text{O}$  values. They have lower  $\delta^{13}\text{C}$  values (-9.6 to -11.2‰) than at Scrivilleri Quarry, which might be due to higher water-rock interaction at the latter. However, with little available data, we cannot exclude that they formed due to vadose percolation with soil-sourced carbon, following the formation of the cave. Considering the small difference (0.5 to 1.5 ‰) in groundwater  $\delta^{18}\text{O}$  values between the Last Glacial and late Holocene estimated for Southern Europe and the Mediterranean (Jasechko et al., 2015), and the 1‰ uncertainty used for the paleowater in our calculation, we think our estimation for the temperature range of calcite formation is reasonable, and does not indicate hydrothermal conditions. In short, the  $\delta^{18}\text{O}$  values do not support a significant hydrothermal source, and likely reflect normal (non-thermal) temperature waters, whilst the  $\delta^{13}\text{C}$  values suggest organic sourced carbon.

### Potential acidic sources

In the absence of any evidence of sulfuric corrosion in the form of secondary replacement gypsum deposits, the most likely source of aggressiveness is carbonic acid, contained in fluids rising through feeders, and locally from bubble trails draining the bedrock. These rising fluids mixed in the phreatic conduits with meteoric water, produce a highly corrosive environment, as evidenced by the flat ceiling notches (Palombara), and the scarcity of underwater calcite deposits associated with the initial phreatic phase. Indeed, ancient speleothems are few and rarely cover the entire walls, while the entrance halls at Monello are only covered with what look like recent stalagmites developed on collapsed blocks.

The only speleothems identified as possibly associated with the initial phreatic phase are the calcite flowstone spar from the Scrivilleri Quarry (SQ.1) covered by a layer of iron oxides, and the calcite vein (MO.15) intersected by the conduit in Monello. The stable isotope values of these calcites are similar to those of more recent speleothems associated with meteoric infiltration and soil-derived  $\text{CO}_2$  (Fig. 10), suggesting a contribution from meteoric water with organic-derived  $\text{CO}_2$ . Interestingly, also more recent speleothems, certainly associated with meteoric infiltration and soil-derived  $\text{CO}_2$  have similar values (Fig. 10).

Other possible deep-seated sources have been considered. Although the present-day volcanism of Etna is nearby (around 60 km to the N), and even more closer the Plio-Quaternary volcanic districts of the Scordia-Lentini basin (25 km to the NW), a volcanic  $\text{CO}_2$  source is unlikely, since the  $\delta^{13}\text{C}$  values of the calcite are more negative than those for volcanic  $\text{CO}_2$  (D'Alessandro et al., 1997). If hydrocarbons from the marly beds of the Ragusa Fm. migrated during tectonic episodes as claimed by Aureli (2000), no isotopic or mineralogical evidence supports such a source. Finally, Pavano et al. (2022) suggest possible upwelling along the extending Avola fault at the end

of each relaxation cycle. This fault is associated with a hot mantle intrusion, and its Pleistocene and recent activity is attested. Similarly, there is little evidence for such a source.

We cannot overlook bubble-trails that significantly predate speleothems and thus could be related to some (past) environmental conditions that are not reflected in the isotopic values of the speleothems. However, while morphological evidence (feeders, bubble trails, etc.) attests to upwelling fluids, the origin of aggressiveness has yet to be precisely determined. We exclude injection of soil-derived  $\text{CO}_2$  at depth, because diffuse infiltration into the porous limestone is expected to be rapidly neutralized by the slowness of the flow, and to be ineffective in producing dissolution at depth. Organic carbon, on the other hand, can be transported deep into the aquifer, getting "trapped" along density boundaries (such as the salt-fresh water boundary, or that between the infiltrating freshwater and resident groundwater). In presence of oxygen this organic carbon can produce  $\text{CO}_2$  and create renewed aggressiveness. Also sulfate-reducing bacteria can reduce sea-water sulfates, forming  $\text{H}_2\text{S}$  that, upon oxidation, can participate in the speleogenetic processes. This latter process, however, if active at some time, did not leave convincing evidence in the investigated caves (e.g., replacement pockets, secondary gypsum deposits). This might easily be explained by the presumable age of caves (between 210 and 330 ka old): sulfuric acid speleogenesis signs might have been lost by successive processes (infiltrating waters, condensation corrosion). We believe that the main source of aggressiveness lies in the freshwater lens on top of the salty water, but this has yet to be demonstrated.

Contributions from aggressive deep-seated fluids with upflowing along major normal faults during phases of tectonic activity, cannot be excluded and should be further investigated.

### Hypogenic speleogenesis related to $\text{CO}_2$ degassing

Apart from a few recent modifications linked to epigenetic evolution (localized introduction of surface sediments by runoff and reworking of lime sands, biocorrosion by bats, and recent localized speleothems), the studied caves show predominantly phreatic morphologies due to slowly moving waters, characteristic of hypogenic activity. The usual epigenetic features, such as scallops and accumulations of fluvial sediments linked to the concentrated runoff from surface water, are lacking. The morphologies attest to rising flows (feeders, vertical phreatic conduits on fractures, wall and ceiling channels, domes) corresponding to the Morphologic Suite of Rising Flow (MSRF, Klimchouk, 2007, 2009). Some deposits, such as massive iron oxides and traces of manganese, could be linked to the transport of metal ions by reduced deep fluids precipitated in contact with meteoric waters due to changing redox conditions. Bubble trails attest to aggressive fluids drained from the bedrock towards the conduits or, more likely, to  $\text{CO}_2$  degassing, the origin of which is not deep, as suggested by stable isotopes. These bubble trails are

preferentially located along major fractures and in the deeper parts of the caves, where they are responsible for the modification of voids in a late phreatic stage. This contribution of continuous aggressiveness is attested by acid notches with a flat upper surface and the absence of underwater speleothems associated with supersaturated water. These observations suggest the existence of aggressive ascending fluids which may have formed the caves. The caves have patterns typical of hypogenic flow: no dendritic structure suggesting the convergence of surface tributaries, but rather maze networks with shafts aligned along fractures, connected by subhorizontal cave fragments sometimes rising along the dip or guided by major fractures, as well as perfectly horizontal levels related to the water table in relation to a stable base level. Given the regional context, such a base level fits well with the corresponding marine level.

Based on the example of Palombara Cave, we propose a speleogenetic model of these karst caves in a coastal area, comparable to flank margin caves (FMC; Fig. 18) (Myrloie & Myrloie, 2007). This model implies the presence of a conduit along major local

discontinuities (faults and bedding planes at the contact of contrasting lithologies), draining meteoric waters diffusely infiltrated into the carbonate matrix, and whose aggressiveness at the beginning of conduit development comes from diffuse input from the matrix (bubble trails) or previously concentrated along fractures (feeders). The flow constraint determined by sea level determines an oblique, upward flow converging towards one or several outlets. The cave pattern thus combines localized zones of vertical or oblique phreatic transfer along fractures terminating upwards in blind chimneys, connected by oblique phreatic conduits along the dip, of reduced size and sometimes anastomosed, as well as horizontal conduits at the water table, all resulting in a maze pattern. Such a configuration falls in the hypogenic type in the sense of Klimchouk (2007).

These are monogenic hypogenic caves due to rising  $\text{CO}_2$ , with elongated cave development at shallow depth below the water table, recording the position of the fresh water lens and hence sea-level position and correlated with marine terraces.

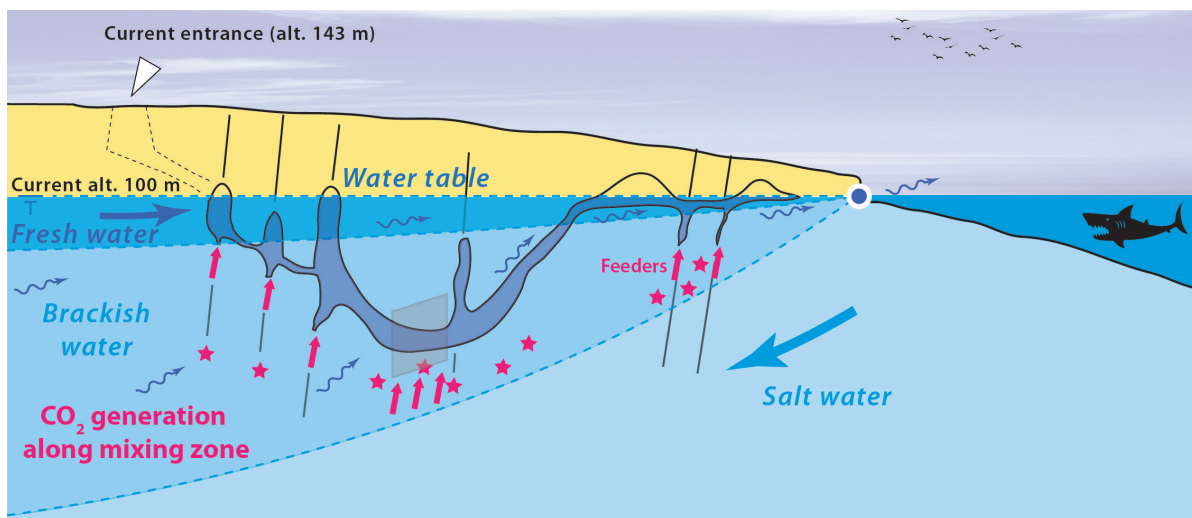


Fig. 18. Flank margin cave (FMC)-type coastal speleogenesis model developed in the shallow phreatic zone, from sources of carbonic aggressivity probably caused by the mixing of waters and oxidation of organic carbon in the mixing zone between fresh and salt water, resulting in a complex cave pattern combining vertical upwellings along fractures, oblique conduits along the dip or fractures, and horizontal conduits at the water table whose altitude is controlled by the contemporary sea level (inspired from Palombara Cave). Note the vertical exaggeration of the thickness of the freshwater lens for clarity of representation.

## CONCLUSIONS

The calcarenite karst of the Syracuse area, which experienced a major Pleistocene uplift, is sculpted by stepped marine terraces that record the position of past sea levels. The studied caves (Palombara, Scrivilleri, Monello) show a clear relationship with these ancient coastal landforms. They present evidence of slow, upward phreatic flows at shallow depths, associated with  $\text{CO}_2$  degassing, thus characteristic of a hypogenic origin. Sediment analysis (mineralogy, stable isotopes) associates Fe and Mn oxide layers with these hypogenic flows, as do calcite spars. For the latter, stable isotopes show a contribution from organic carbon, with formation temperature comparable to the present, thus ruling out any hydrothermal contribution, as well as any deep-seated aggressive input associated with nearby sources, whether volcanic, hydrocarbon or mantle fluids

expelled during regional fault motion. Other types of sediment are related to late speleogenetic phases when caves were exposed by erosion to the surface. These include fine allogenic materials introduced by runoff and deposited in low-lying areas, speleothems formed by supersaturated infiltration, and minerals (phosphates, kaolinite and montmorillonite) derived from the acid decay of bat guano reacting with the host rock and allogenic clays. Added to this are thick deposits of lime sand, resulting from the disaggregation of calcarenite walls by biocorrosion-activated condensation, directly at the foot of the walls or reworked into stratified accumulations by run-off. Active drip holes up to 70 cm deep cutting into speleothems and boulders are most probably the result of intense biocorrosion. Although we have no drip water chemistry, the large quantities of guano and bats in the cave, and the reduced vegetation and soil cover attested since at least 4,500 years indicate

guano- and bat-derived acidity as the most probable sources of fluid aggressivity.

The morphology of these caves attests to slow ascending flows, entering low points and rising vertically along fractures or obliquely along stratigraphic interfaces, shaping typical Morphologic Suites of Rising Flow (MSRF), with from bottom to top: feeders, wall and ceiling channels, and domes. These hypogenic flow morphologies are complemented by features typical of CO<sub>2</sub> degassing: in the deep zones, bubble trails and acid notches at the top of the water table. The caves are organized in a maze pattern, alternating vertical or oblique conduits guided by fractures and gently rising galleries following stratigraphic interfaces. Some perfectly horizontal conduits, where the acid notches are found, record the precise position of the water table, itself dependent on the contemporary sea level. For all these reasons, we propose a speleogenetic model for these hypogenic caves of the Flank Margin (FMC) type, whose aggressiveness would be mainly produced by the mixing of fresh and salt waters, the oxidation of surface-derived organic carbon in the freshwater lens density interfaces, and the possible bacterially-mediated reduction of marine sulfates into H<sub>2</sub>S (the oxidation creates sulfuric acid, which reacts with limestone to produce extra CO<sub>2</sub>). Diffuse water flow in the calcarenites would then transport the solutes from the onshore plateaus to the sea.

At Palombara Cave, U/Th dating of sediments sealing a nearby marine notch, as well as clay sediments bearing paleomagnetic inversions, yielded ages of 603 ± 182 ka and >780 ka, respectively. These ages are significantly older than those calculated by extrapolation from earlier dating of lower altitude marine terraces. Beyond the reliability of the ages we have obtained, the discussion raises the question of the chronology of the high marine terraces derived from extrapolation of age models, but also of the age of the coastal FMC, which could have been established at periods of earlier low marine levels. Future studies will need to address these complex chronological aspects, as well as characterizing the generation of carbonic aggressivity in the mixing zone of the coastal groundwater and its role in the speleogenesis of such FMC.

## ACKNOWLEDGEMENTS

Elena Amore, Salvatore Costanzo, and Fabio Branca, directors of the Integral Nature Reserves of Grotta Palombara and Grotta Monello caves, are thanked for granting access to the caves. The two natural reserves are currently managed by the "Area della Terza Missione" office of the Catania University, in the framework of the system of protected natural areas of the Sicilian Region. Gaetano Guidice and Giuseppe Spitaleri, explorers of Scivilleri Cave, provided cave survey data. Cavers of Le Taddarite speleological association are thanked to the field support. FG acknowledges the Ramón y Cajal fellowship, RYC2020-029811-I and the grant PPIT-UAL, Junta de Andalucía-FEDER 2022-2026 (RyC-

PPI2021-01). We are indebted to John Mylroie, Arthur and Margaret Palmer and an anonymous reviewer for their useful comments and corrections that greatly improved our paper.

**Authorship statement:** PA participated in field work, manage the project, acquired funding, performed microscopic description of samples, designed the study, wrote and reviewed the manuscript with contributions from all co-authors; JYB participated in field work; DC participated in field work and performed 3D photogrammetry of the drip holes; PC conducted palaeomagnetic research; IMDA, GK, JCN participated in field work and reviewed the manuscript; HC and RLE performed U/Th dating; FGS performed stable-isotope analysis and reviewed the manuscript; GM and MV participated in field work, managed the project, acquired funding, and reviewed the manuscript; MT participated in field work, performed stable-isotope analysis and reviewed the manuscript; JDW participated in field work, wrote and reviewed the manuscript.

## REFERENCES

- Antonoli, F., Kershaw, S., Renda, P., Rust, D., Belluomini, G., Cerasoli, M., Radtke, U., Silenzi, S., 2006. Elevation of the last interglacial highstand in Sicily (Italy): a benchmark of coastal tectonics. *Quaternary International*, 145–146, 3–18. <https://doi.org/10.1016/j.quaint.2005.07.002>
- Arena, L., Bongiorno, C., Castorina, R., Giudice, G., Iemmolo, A., Sequenzia, M., Spitaleri, G., 2013. Scivilleri: cronaca di una grotta annunciata. *V Congresso Regionale di Speleologia della Sicilia*, 1–7.
- Aricò, P., Vattano, M., 2007. Primo contributo sui depositi a "terra rossa" dell'Abisso del Vento, Isnello (PA). *Speleologia Iblea*, 12, 79–84. <https://www.researchgate.net/publication/235653964>
- Audra, P., Mocochain, L., Bigot, J.-Y., Nobécourt, J.-C., 2009a. The association between bubble trails and folia: A morphological and sedimentary indicator of hypogenic speleogenesis by degassing, example from Adaouste Cave (Provence, France). *International Journal of Speleology*, 38(2), 93–102. <http://dx.doi.org/10.5038/1827-806X.38.2.1>
- Audra, P., Mocochain, L., Bigot, J.-Y., Nobécourt, J. C. 2009b. Morphological indicators of speleogenesis: hypogenic speleogens. *Hypogenic Speleogenesis and Karst Hydrogeology of Artesian Basins*, Chernivtsy, 23–32. Ukrainian Institute of Speleology and Karstology, Simferopol, Ukraine.
- Audra, P., Palmer, A. N., 2013. The vertical dimension of karst. Controls of vertical cave pattern. In: Shroder, J. (Ed.), *Treatise on geomorphology*, vol. 6 (Karst geomorphology), 186–206. Elsevier Inc., Academic Press, San Diego. <http://dx.doi.org/10.1016/B978-0-12-374739-6.00098-1>
- Audra, P., Bigot, J.Y., De Waele, J., Madonia, G., Nobécourt, J.-C., Vattano, M., 2012. Hypogenic caves in Sicily. 20th International Karst School "Caves – exploration and studies", Postojna. Karst Research Institute (IZRK), Poster. <http://dx.doi.org/10.13140/RG.2.2.28043.26407>
- Audra, P., Bigot, J.-Y., De Waele, J., Galli, E., Madonia, G., Nobécourt, J.-C., Scopelliti, G., Vattano, M.,

2015. Update on the hypogenic caves of Sicily. 23th International Karst School "Karst forms and processes", Postojna. Karst Research Institute (IZRK), Poster. <http://dx.doi.org/10.13140/RG.2.2.12943.76969>
- Audra, P., Barriquand, L., Bigot, J.-Y., Cailhol, D., Caillaud, H., Vanara, N., Nobécourt, J.-C., Madonia, G., Vattano, M., Renda, M. 2016. L'impact méconnu des chauves-souris et du guano dans l'évolution morphologique tardive des cavernes. *Karstologia*, 68, 1-20. <https://www.researchgate.net/publication/326147747>
- Audra, P., Barriquand, L., Bigot, J.-Y., Cailhol, D., Caillaud, H., Vanara, N., Nobécourt, J.-C., Madonia, G., Vattano, M., 2017. The little-known impact of bats and bat guano in the late stages of cave morphogenesis. 25th International Karst School "Milestones and challenges in karstology", Postojna. <https://www.researchgate.net/publication/317528121>
- Audra, P., De Waele, J., Bentaleb, I., Chronáková, A., Křišťufek, V., D'Angeli, I.M., Carbone, C., Madonia, G., Vattano, M., Scopelliti, G., Cailhol, D., Vanara, N., Temovski, M., Bigot, J.-Y., Nobécourt, J.-C., Galli, E., Rull, F., Sanz-Arranz, A., 2019. Guano-related phosphates-rich minerals in European caves. *International Journal of Speleology*, 48(1), 75-105. <https://doi.org/10.5038/1827-806X.48.1.2252>
- Audra, P., Heresanu, V., Barriquand, L., El Kadiri Boutchich, M., Jailliet, S., Pons-Branchu, E., Bosák, P., Cheng, H., Edwards, R.L., Renda, M., 2021. Bat guano minerals and mineralization processes in Chameau Cave, Eastern Morocco. *International Journal of Speleology*, 50(1), 91-109. <https://doi.org/10.5038/1827-806X.50.1.2374>
- Aureli, A., 2000. Il carsismo nei calcari di piattaforma e i rapporti con la tettonica e gli idrocarburi risalenti da giacimenti profondi. *Speleologia Iblea*, 8, 73.
- Bada, J.L., Belluomini, G., Bonfiglio, L., Branca, M., Burgio, E., Dellitala, L., 1991. Isoleucine Epimerization ages of quaternary mammals of Sicily. *Il Quaternario*, 4(1), 49-54. <https://www.researchgate.net/publication/283737170>
- Badino, G., Torelli L., 2014. The "Progetto Kronio": history and problems of an extreme exploration in an intact archaeological deposit. In: Gulli, D. (Ed.), *From cave to dolmen: Ritual and symbolic aspects in the prehistory between Sciacca, Sicily and the central Mediterranean*, Archaeopress, p. 31-42. <https://doi.org/10.2307/j.ctvqmp11h.6>
- Barriquand, L., Bigot, J.-Y., Audra, P., Cailhol, D., Gauchon, C., Heresanu, V., Jailliet, S., Vanara, N., 2021. Caves and Bats: morphological impacts and archaeological consequences. The Azé Prehistoric Cave (Saône-et-Loire, France). *Geomorphology*, 388, 107785. <https://doi.org/10.1016/j.geomorph.2021.107785>
- Bianca, M., Monaco, C., Tortorici, L., Cernobori, L., 1999. Quaternary normal faulting in southeastern Sicily (Italy): a seismic source for the 1693 large earthquake. *Geophysical Journal International*, 139(2), 370-394. <https://doi.org/10.1046/j.1365-246x.1999.00942.x>
- Billi, A., Barberi, G., Faccenna, C., Neri, G., Pepe, F., Sulli, A., 2006. Tectonics and seismicity of the Tindari Fault System, southern Italy: Crustal deformations at the transition between ongoing contractional and extensional domains located above the edge of a subducting slab. *Tectonics* 25, TC2006. <https://doi.org/10.1029/2004TC001763>
- Bonfiglio, L., Rosso, A., Herridge, V., Insacco, G., Reitano, A., Minniti, G., Mangano, G., Sanfilippo, R., 2022. Pleistocene caves of Eastern Sicily coast: exceptional archives to reconstruct the history of the island's biota. *Geosciences*, 12(7), 258. <https://doi.org/10.3390/geosciences12070258>
- Bonforte, A., Catalano, S., Maniscalco, R., Pavano, F., Romagnoli, G., Sturiale, G., Tortorici, G., 2015. Geological and geodetic constraints on the active deformation along the northern margin of the Hyblean Plateau (SE Sicily). *Tectonophysics*, 640, 80-89. <https://doi.org/10.1016/j.tecto.2014.11.024>
- Bottrell, S.H., Carew, J.L., Mylroie, J.E., 1993. Bacterial sulphate reduction in flank margin environments: evidence from sulphur isotopes. In: White, W.B. (Ed.), *Proceedings of the 6th Symposium on the geology of the Bahamas*, Port Charlotte, Florida, Bahamian Field Station, p. 17-21.
- Breithaupt, C.I., Gulley, J.D., Bunge, E.M., Moore, P.J., Kerans, C., Fernandez-Ibanez, F., Fullmer, S.M., 2022. A transient, perched aquifer model for banana hole formation: evidence from San Salvador Island, Bahamas. *Earth Surface Processes and Landforms*, 47, 618-638. <https://doi.org/10.1002/esp.5276>
- Burford, E.P., Kierans, M., Gadd, G.M. 2003. Geomycology: fungi in mineral substrata. *Mycologist*, 17(3), 98-107. <https://doi.org/10.1017/S0269915X03003112>
- Butler, R.W., Maniscalco, R., Pinter, P.R., 2019. Syn-kinematic sedimentary systems as constraints on the structural response of thrust belts: re-examining the structural style of the Maghrebian thrust belt of Eastern Sicily. *Italian Journal of Geosciences*, 138 (3), 371-389. <https://doi.org/10.3301/IJG.2019.11>
- Cailhol, D., Audra, P., Nehme, C., Nader, F.H., Garašić, M., Heresanu, V., Gucel, S., Charalambidou, I., Satterfield, L., Cheng, H., Edwards, R.L., (2019). The contribution of condensation-corrosion in the morphological evolution of caves in semi-arid regions: preliminary investigations in the Kyrenia Range, Cyprus. *Acta Carsologica*, 48(1), 5-27. <https://doi.org/10.3986/ac.v48i1.6782>
- Carbone, S., Di Geronimo, I., Grasso, M., Iozzia, S., Lentini, F., 1982. I terrazzi marini quaternari dell'area Iblea (Sicilia SW). Contributi conclusivi per la realizzazione della carta Neotettonica d'Italia. *Progetto Finalizzato geodinamica*, 506, 35 p.
- Catalano, S., Romagnoli, G., Tortorici, G., 2010. Kinematics and dynamics of the late quaternary rift-flank deformation in the Hyblean Plateau (SE Sicily). *Tectonophysics*, 486, 1-14. <https://doi.org/10.1016/j.tecto.2010.01.013>
- Catalano, R., Valenti, V., Albanese, C., Accaino, F., Sulli, A., Tinivella, U., Gasparo Morticelli, M., Zanolta, C., Giustiniani, M., 2013. Sicily's fold/thrust belt and slab rollback: The SI.RI.PRO. seismic crustal transect. *Journal of the Geological Society of London*, 170, 451-464. <https://doi.org/10.1144/jgs2012-099>
- Cheng, H., Edwards, R.L., Shen, C.-C., Polyak, V.J., Asmerom, Y., Woodhead, J., Hellstrom, J., Wang, Y., Kong, X., Spötl, C., Wang, X., Alexander, E.C., 2013. Improvements in <sup>230</sup>Th dating, <sup>230</sup>Th and <sup>234</sup>U half-life values, and U-Th isotopic measurements by multi-collector inductively coupled plasma mass spectrometry. *Earth and Planetary Science Letters* 371-372, 82-91. <https://doi.org/10.1016/j.epsl.2013.04.006>
- Chiesa, M., Forti, P., 1987. Studio morfologico di due nuove cavità carsiche dell'Iglesiente (Sardegna Sud occidentale). *Ipoantropo*, 4, 40-45 Reggio Emilia, Italia. <https://www.researchgate.net/publication/281574941>
- Chiarabba, C., De Gori, P., Speranza, F., 2008. The

- southern Tyrrhenian subduction zone: deep geometry, magmatism and Plio-Pleistocene evolution. *Earth and Planetary Science Letters*, 268, 408–423.  
<https://doi.org/10.1016/2008.01.036>
- Columbu, A., Chiarini, V., Spötl, C., Benazzi, S., Hellstrom, J., Cheng, H., De Waele, J. 2020. Speleothem record attests to stable environmental conditions during Neanderthal–modern human turnover in southern Italy. *Nature Ecology & Evolution*, 4, 1188–1195.  
<https://doi.org/10.1038/s41559-020-1243-1>
- Daëron, M., Drysdale, R.N., Peral, M., Huyghe, D., Blamart, D., Coplen, T.B., Lartaud, F., Zanchetta, G., 2019. Most Earth-surface calcites precipitate out of isotopic equilibrium. *Nature Communications*, 10(1), 429. <https://doi.org/10.1038/s41467-019-08336-5>
- D'Alessandro, W., Giammanco, S., Parello, F., Valenza, M., 1997. CO<sub>2</sub> output and δ<sup>13</sup>C(CO<sub>2</sub>) from Mount Etna as indicators of degassing of shallow asthenosphere. *Bulletin of Volcanology*, 58, 455–458.  
<https://doi.org/10.1007/s004450050154>
- D'Angeli, I.M., 2019. Speleogenesis of sulfuric acid caves in southern Italy. Unpublished PhD Thesis, University of Bologna.  
<https://doi.org/10.48676/unibo/amsdottorato/9022>
- D'Angeli, I. M., Sanna, L., Calzoni, C., De Waele, J., 2015. Uplifted flank margin caves in telogenetic limestones in the Gulf of Orosei (Central-East Sardinia—Italy) and their palaeogeographic significance. *Geomorphology*, 231, 202–211.  
<https://doi.org/10.1016/j.geomorph.2014.12.008>
- D'Angeli, I.M., Carbone, C., Nagostinis, M., Parise, M., Vattano, M., Madonia, G., De Waele, J., 2018. New insights on secondary minerals from Italian sulfuric acid caves. *International Journal of Speleology*, 47(3), 271–191.  
<https://doi.org/10.5038/1827-806X.47.3.2175>
- D'Angeli, I.M., Parise, M., Vattano, M., Madonia, G., Galdenzi, S., De Waele, J., 2019. Sulfuric acid caves of Italy: A review. *Geomorphology*, 333, 105–122.  
<http://dx.doi.org/10.1016/j.geomorph.2019.02.025>
- D'Angeli, I.M., Nagostinis, M., Carbone, C., Bernasconi, S.M., Polyak, V.J., Peters, L., McIntosh, W., De Waele, J., 2019b. Sulfuric acid speleogenesis in the Majella Massif (Abruzzo, Central Apennines, Italy). *Geomorphology*, 333, 167–179.  
<https://doi.org/10.1016/j.geomorph.2019.02.036>
- De Martini, P.M., Barbano, M.S., Pantosti, D., Smedile, A., Pirrotta, C., Del Carlo, P., Pinzi, S., 2012. Geological evidence for paleotsunamis along eastern Sicily (Italy): an overview. *Natural Hazards and Earth System Sciences*, 12(8), 2569–2580.  
<https://doi.org/10.5194/nhess-12-2569-2012>
- De Waele, J., Gutiérrez, F., 2022. Karst hydrogeology, geomorphology and caves. John Wiley & Sons, Chichester, 888 p.
- De Waele, J., Galdenzi, S., Madonia, G., Menichetti, M., Parise, M., Piccini, L., Sanna, L., Sauro F., Tognini, P., Vattano, M., Vigna, B., 2014. A review on hypogene caves in Italy. In: Klimchouk, A.B., Sasowsky, I., Mylroie, J., Engel, S.A., Engel, A.S. (Eds.), *Hypogene cave morphologies*. Karst Waters Institute Special Publication 18, Leesburg, Virginia, p. 28–30.  
[http://karstwaters.org/wp-content/uploads/2015/04/SP18\\_Hypogene1.pdf](http://karstwaters.org/wp-content/uploads/2015/04/SP18_Hypogene1.pdf)
- De Waele, J., Audra, P., Madonia, G., Vattano, M., Plan, L., D'Angeli, I.M., Bigot, J.-Y., Nobécourt, J.-C., 2016. Sulfuric acid speleogenesis (SAS) close to the water table: Examples from southern France, Austria, and Sicily. *Geomorphology*, 253, 452–467.  
<http://dx.doi.org/10.1016/j.geomorph.2015.10.019>
- De Waele, J., D'Angeli, I.M., Audra, P., Plan L., Palmer, A.N., 2024. Sulfuric acid caves of the world: a review. *Earth-Science Reviews*, 250, 104693.  
<https://doi.org/10.1016/j.earscirev.2024.104693>
- Di Grande, A., Raimondo, W., 1982. Linee di costa plio-pleistoceniche e schema litostratigrafico del Quaternario siracusano. *Geologica Romana*, 21, 279–309.  
[https://www.dst.uniroma1.it/geologicaromana/Volumi/VOL%2021/GR\\_21\\_279\\_309\\_DI%20Grande%20et%20al.pdf](https://www.dst.uniroma1.it/geologicaromana/Volumi/VOL%2021/GR_21_279_309_DI%20Grande%20et%20al.pdf)
- Di Maggio, C., Madonia, G., Parise, M., Vattano, M., 2012. Karst of Sicily and its conservation. *Journal of Cave and Karst Studies*, 74, 157–172.  
<https://dx.doi.org/10.4311/2011JCKS0209>
- Di Piazza, S., Isaia, M., Vizzini, A., Badino, G., Voyron, S., Zotti, M., 2017. First mycological assessment in hydrothermal caves of Monte Kronio (Sicily, southern Italy). *Webbia*, 72(2), 277–285.  
<https://doi.org/10.1080/00837792.2017.1347368>
- Distefano, S., Gamberi, F., Baldassini, N., Di Stefano, A., 2021. Quaternary evolution of coastal plain in response to sea-level changes: Example from south-east Sicily (Southern Italy). *Water*, 13, 1524.  
<https://doi.org/10.3390/w13111524>
- Dogliani, C., Gueguen, E., Harabaglia, P., Mongelli, F., 1999. On the origin of west-directed subduction zones and applications to the western Mediterranean. In: Durand, B., Jolivet, L., Horváth, F., Séranne, M. (Eds.), *The Mediterranean basins: Tertiary extension within the Alpine Orogen*. Geological Society, London, Special Publications, 156, 541–561.  
<https://doi.org/10.1144/GSL.SP.1999.156.01.24>
- Dutton, A., Scicchitano, G., Monaco, C., Desmarchelier, J.M., Antonioli, F., Lambeck, K., Esat, T.M., Fifield, L.K., McCulloch, M.T., Mortimer, G., 2009. Uplift rates defined by U-series and <sup>14</sup>C ages of serpulid-encrusted speleothems from submerged caves near Siracusa, Sicily (Italy). *Quaternary Geochronology*, 4, 2–10.  
<https://dx.doi.org/10.1016/j.quageo.2008.06.003>
- Faccenna, C., Piromallo, C., Crespo-Blanc, A., Jolivet, L., Rosetti, F., 2004. Lateral slab deformation and the origin of the western Mediterranean arcs. *Tectonics*, 23, TC1012. <https://doi.org/10.1029/2002TC001488>
- Ford, D.C., Williams, P.D., 2007. Karst hydrogeology and geomorphology. John Wiley & Sons, Chichester, 562 p.
- Fornós, J.J., Merino, A., Ginés, J., Ginés, A., Gracia F., 2011. Solutional features and cave deposits related to hypogene speleogenetic processes in a littoral cave of Mallorca Island (western Mediterranean). *Carbonates and Evaporites*, 26, 69–81.  
<https://doi.org/10.1007/s13146-010-0040-3>
- Fratesi, B., 2013. Hydrology and geochemistry of the freshwater lens in coastal karst. In: Lace, M.J., Mylroie, J.E. (Eds.), *Coastal karst landforms*. Coastal Research Library 5, Springer, Dordrecht, p. 59–75.
- Frisia, S., Borsato, A., Mangini, A., Spötl, C., Madonia, G., & Sauro, U., 2006. Holocene climate variability in Sicily from a discontinuous stalagmite record and the Mesolithic to Neolithic transition. *Quaternary Research*, 66(3), 388–400.  
<https://doi.org/10.1016/j.yqres.2006.05.003>
- Gázquez, F., Columbu, A., De Waele, J., Breitenbach, S.F., Huang, C.R., Shen, C.C., Lu, Y., Calaforra, J.-C., Mleneck-Vautravers, M.J., Hodell, D.A., 2018. Quantification of paleoaquifer changes using clumped isotopes in subaqueous carbonate speleothems. *Chemical Geology*, 493, 246–257.

- <https://doi.org/10.1016/j.chemgeo.2018.05.046>
- Gulley, J.D., Martin, J.B., Moore, P.J., Brown, A., Spellman, P.D., Ezell, J., 2015. Heterogeneous distributions of CO<sub>2</sub> may be more important for dissolution and karstification in coastal eogenetic limestone than mixing dissolution. *Earth Surface Processes and Landforms*, 40(8), 1057-1071. <https://doi.org/10.1002/esp.3705>
- Henriquet, M., Dominguez, S., Barreca, G., Malavieille, J., Cadio, C., Monaco, C., 2019. Deep origin of the dome-shaped Hyblean Plateau, Southeastern Sicily: A new tectono-magmatic model. *Tectonics* 38 (12), 4488–4515. <https://doi.org/10.1029/2019TC005548>
- Jaffey, A.H., Flynn, K.F., Glendenin, L.E., Bentley, W.C., Essling, A.M., 1971. Precision measurement of half-lives and specific activities of <sup>235</sup>U and <sup>238</sup>U. *Physical Review C*, 4(5), 1889–1906. <https://doi.org/10.1103/PhysRevC.4.1889>
- Jasechko, S., Lechler, A., Pausata, F. S. R., Fawcett, P. J., Gleeson, T., Cendón, D. I., Galewsky, J., LeGrande, A. N., Risi, C., Sharp, Z. D., Welker, J. M., Werner, M., and Yoshimura, K. 2015. Late-glacial to late-Holocene shifts in global precipitation δ<sup>18</sup>O. *Climate of the Past*, 11, 1375–1393. <https://doi.org/10.5194/cp-11-1375-2015>
- Klimchouk, A.B. 2007. Hypogene speleogenesis: hydrogeological and morphogenetic perspective. Special Paper no. 1, National Cave and Karst Research Institute, Carlsbad, New Mexico, 106 p.
- Klimchouk, A.B., 2009. Morphogenesis of hypogenic caves. *Geomorphology*, 106, 100–117. <https://doi.org/10.1016/j.geomorph.2008.09.013>
- Klimchouk, A.B., Ford, D.C., Palmer, A.N., Dreybroth, W. (Eds.), 2000. Speleogenesis, evolution of karst aquifers. National Speleological Society, Huntsville, Alabama.
- Klimchouk, A.B., Sasowsky, I., Mylroie, J., Engle, S.A., Engle, A.S. (Eds.), 2014. Hypogene cave morphologies. Karst Waters Institute Special Publication 18, Karst Waters Institute, Leesburg, Virginia, 111 p.
- Lentini, F., Carbone, S., 2014. The foreland domain. *Geology of Sicily. Memorie Descrittive della Carta Geologica d'Italia*, 95, 1-409. [https://www.isprambiente.gov.it/it/pubblicazioni/periodici-tecnici/memorie-descrittive-della-carta-geologica-ditalia/memdes\\_95\\_avampaese.pdf](https://www.isprambiente.gov.it/it/pubblicazioni/periodici-tecnici/memorie-descrittive-della-carta-geologica-ditalia/memdes_95_avampaese.pdf)
- Lentini, F., Carbone, S., Catalano, S., 1994. Main structural domains of the central Mediterranean region and their Neogene tectonic evolution. *Bollettino di Geofisica Teorica ed Applicata*, 36, 103-126. <https://bgo.ogs.it/issues/1994-vol-36-141-144/main-structural-domains-central-mediterranean-region-and-their-neogene>
- López-Martínez, R., Gázquez, F., Calaforra, J.M., Audra, P., Bigot, J.Y., Pi Puig, T., Alcántara, R., Navarro, A., Crochet, R., Corona-Martínez, L., Daza Brunet, R., 2020. Bubble trail and folia in cenote Zapote, Mexico: petrographic evidence for abiotic precipitation driven by CO<sub>2</sub> degassing below the water table. *International Journal of Speleology*, 49(3), 173-186. <https://doi.org/10.5038/1827-806X.49.3.2344>
- Lugli, S., Rosario, R., Riccardo, O., Giorgio, S., 2017. Grotta dell'Acqua Mintina a peculiar geosite with the smell of sulfur. *Speleologia Iblea*, 16, 65-71.
- Magny, M., Vannièrè, B., Calò, C., Millet, L., Leroux, A., Peyron, O., Zanchetta, G., La Mantia, T., Tinner, W., 2011. Holocene hydrological changes in south-western Mediterranean as recorded by lake-level fluctuations at Lago Preola, a coastal lake in southern Sicily, Italy. *Quaternary Science Reviews*, 30(19-20), 2459-2475. <https://doi.org/10.1016/j.quascirev.2011.05.018>
- Marziano, C., Chilardi, S., 2005. Contribution to knowledge of the Pleistocene mammal-bearing deposits of Siracusa (Southeastern Sicily). In: O'Connor T. (Ed.), *Biosphere to lithosphere*, 94-109, Oxbow Books, Oxford. <https://www.researchgate.net/publication/301636473>
- Meschis, M., Scicchitano, G., Roberts, G. P., Robertson, J., Barreca, G., Monaco, C., Spampinato C., Sahy, D., Antonioli, F., Mildon, S.K., Scardino, G., 2020. Regional deformation and offshore crustal local faulting as combined processes to explain uplift through time constrained by investigating differentially uplifted late quaternary paleoshorelines: The foreland Hyblean plateau, SE Sicily. *Tectonics*, 39(12), e2020TC006187. <https://doi.org/10.1029/2020TC006187>
- Meschis, M., Roberts, G.P., Robertson, J., Mildon, Z.K., Sahy, D., Goswami, R., Sgambato, C., Faure Walker, J., Michetti, A.M., Iezzi, F., 2022. Out of phase Quaternary uplift-rate changes reveal normal fault interaction, implied by deformed marine palaeoshorelines. *Geomorphology*, 416, 108432. <https://doi.org/10.1016/j.geomorph.2022.108432>
- Michelangeli, F., Di Rita, F., Celant, A., Tisnérat-Laborde, N., Lirer, F., Magri, D., 2022. Three millennia of vegetation, land-use, and climate change in SE Sicily. *Forests*, 13(1), 102. <https://doi.org/10.3390/f13010102>
- Montheil, L., Philippon, M., Münch, P., Camps, P., Vaes, B., Cornée, J.J., Poidras, T., van Hinsbergen D.J.J., 2023. Paleomagnetic rotations in the northeastern Caribbean region reveal major intraplate deformation since the Eocene. *Tectonics*, 2023, 42 (8). <https://doi.org/10.1029/2022TC007706>
- Mylroie, J.E., 2013. Coastal karst development in carbonate rocks. In: Lace, M.J., Mylroie, J.E. (Eds.), *Coastal karst landforms*. Coastal Research Library 5, Springer, Dordrecht, p. 77-109.
- Mylroie, J.E., Carew, J.L., 1990. The flank margin model for dissolution cave development in carbonate platforms. *Earth Surface Processes and Landforms*, 15(5), 413-424. <https://doi.org/10.1002/esp.3290150505>
- Mylroie, J.E., Mylroie, J.R., 2007. Development of the Carbonate Island Karst Model. *Journal of Cave and Karst Studies*, 69(1), 59-75. <https://legacy.caves.org/pub/journal/PDF/v69/cave-69-01-59.pdf>
- Mylroie, J.E., Mylroie, J.R., 2009. Diagnostic features of hypogenic karst: Is confined flow necessary? In: Stafford, K.W., Land, L., Veni, G. (Eds.), *Advances in hypogene karst studies: NCKRI Symposium 1*. National Cave and Karst Research Institute, Carlsbad, New Mexico, p. 12-26.
- Mylroie, J.E., Mylroie, J.R., 2013. Telogenetic limestones and island karst. In: Lace, M.J., Mylroie, J.E., (Eds.), *Coastal karst landforms*. Coastal Research Library 5, Springer, Dordrecht, p. 375-393.
- Mylroie, J.E., Mylroie, J.R., Nelson, C.S., 2008. Flank margin cave development in telogenetic limestones of New Zealand. *Acta Carsologica*, 37(1), 15-40. <https://doi.org/10.3986/ac.v37i1.157>
- Onac, B.P., Mylroie, J.E., White, W.B., 2001. Mineralogy of cave deposits on San Salvador Island, Bahamas. *Carbonates and Evaporites*, 16(1), 8-16. <https://doi.org/10.1007/BF03176222>
- Otoničar, B., Buzjak, N., Mylroie, J.E., 2010. Flank margin cave development in carbonate talus breccia facies: an example from Cres island, Croatia. *Acta carsologica*, 39(1), 79-91. <https://doi.org/10.3986/ac.v39i1.114>

- Palmer, A.N., 1991. Origin and morphology of limestone caves. *Geological Society of America Bulletin*, 103(1), 1-21.  
[https://doi.org/10.1130/0016-7606\(1991\)103<0001:OAMOLC>2.3.CO;2](https://doi.org/10.1130/0016-7606(1991)103<0001:OAMOLC>2.3.CO;2)
- Palmer, A.N., 2000. Hydrogeological control of cave patterns. In: Klimchouk, A.B., Palmer, A.N., Ford, D.C., Dreybrodt, W. (Eds.), *Speleogenesis: Evolution of karst aquifers*, National Speleological Society, Huntsville, p. 77-90.
- Pavano, F., Romagnoli, G., Tortorici, G., Catalano, S., 2019. Morphometric evidences of recent tectonic deformation along the southeastern margin of the Hyblean Plateau (SE-Sicily, Italy). *Geomorphology*, 342, 1-19.  
<https://doi.org/10.1016/j.geomorph.2019.06.006>
- Pavano, F., Tortorici, G., Romagnoli, G., Catalano, S., 2022. Age attribution to a karst system using river long profile analysis (Hyblean Plateau, Sicily, Italy). *Geomorphology*, 400, 108095.  
<https://doi.org/10.1016/j.geomorph.2021.108095>
- Pedley, M., Grasso, M., 1992. Miocene syntectonic sedimentation along the western margins of the Hyblean-Malta platform: a guide to plate margin processes in the central Mediterranean. *Journal of Geodynamics*, 15(1-2), 19-37.  
[https://doi.org/10.1016/0264-3707\(92\)90004-C](https://doi.org/10.1016/0264-3707(92)90004-C)
- Piatanesi, A., Tinti, S., 1998. A revision of the 1693 eastern Sicily earthquake and tsunami. *Journal of Geophysical Research: Solid Earth*, 103(B2), 2749-2758. <https://doi.org/10.1029/97JB03403>
- Piccini, L., De Waele, J., Galli, E., Polyak, V. J., Bernasconi, S. M., Asmerom, Y., 2015. Sulphuric acid speleogenesis and landscape evolution: Montecchio cave, Albegna river valley (Southern Tuscany, Italy). *Geomorphology*, 229, 134-143.  
<https://doi.org/10.1016/j.geomorph.2014.10.006>
- Pitman S.D.M.D., 2010. Amino acid racemization dating. <https://www.detectingdesign.com/aminoacid dating.html>
- Plan, L., Tschegg, C., De Waele, J., Spötl, C., 2012. Corrosion morphology and cave wall alteration in an Alpine sulfuric acid cave (Kraushöhle, Austria). *Geomorphology*, 169-170, 45-54.  
<https://doi.org/10.1016/j.geomorph.2012.04.006>
- Polyak, V. J., McIntosh, W. C., Guven, N., Provencio, P., 1998. Age and origin of Carlsbad Cavern and related caves from  $^{40}\text{Ar}/^{39}\text{Ar}$  of alunite. *Science*, 279, 1919-1922. <https://doi.org/10.1126/science.279.5358.191>
- Polyak, V.J., Provencio, P.P., Asmerom, Y., Davis, D.G., Onac, B.P., Palmer, A.N., Palmer, M.V., 2022. Timing of sulfuric acid speleogenesis (SAS) as an indicator of canyon incision rates of the Shoshone and Bighorn rivers, Wyoming, USA. *Geomorphology*, 410, 108281.  
<https://doi.org/10.1016/j.geomorph.2022.108281>
- Powell J., Collins M.J., Cussens J., MacLeod N., Penkman K.E.H., 2013. Results from an amino acid racemization inter-laboratory proficiency study; design and performance evaluation, *Quaternary Geochronology*, 16, 183-197.  
<https://doi.org/10.1016/j.quageo.2012.11.001>
- Ruggieri, R., Amore, C., 2000. Elementi geostrutturali e paleomorfologici del sistema carsico grotta Monello (Sicilia sud-orientale). *Speleologia Iblea*, 8, 75-81.
- Ruggieri, R., De Waele, J., 2014. Lower-to Middle Pleistocene flank margin caves at Custonaci (Trapani, NW Sicily) and their relation with past sea levels. *Acta Carsologica*, 43(1), 11-22.  
<https://doi.org/10.3986/ac.v43i1.899>
- Ruggieri, R., Nastasi, C., Zammitti, P. 2000. Geostrutture e morfologie della grotta Palombara (Sicilia sud-orientale). *Speleologia Iblea*, 8, 197-205.
- Ruggieri, R., Zocco, M., 2000. Il carsismo dell'area grotta Perciata-Chiusazza (Sicilia sudorientale): morfostrutture e speleogenesi. *Speleologia Iblea*, 8, 169-185.
- Sadori, L., Ortu, E., Peyron, O., Zanchetta, G., Vannièrè, B., Desmet, M., & Magny, M., 2013. The last 7 millennia of vegetation and climate changes at Lago di Pergusa (central Sicily, Italy). *Climate of the Past*, 9(4), 1969-1984. <https://doi.org/10.5194/cp-9-1969-2013>
- Schiavo, M.A., Hauser, S., Povinec, P.P. 2009. Stable isotopes of water as a tool to study groundwater-seawater interactions in coastal south-eastern Sicily. *Journal of Hydrology*, 364(1-2), 40-49.  
<https://doi.org/10.1016/j.jhydrol.2008.10.005>
- Scicchitano, G., Antonioli, F., Castagnino Berlinghieri, E.F., Dutton, A., Monaco, C., 2008. Submerged archaeological sites along the Ionian Coast of south-eastern Sicily and implications with the Holocene relative sea level change. *Quaternary Research*, 70, 26-39. <https://doi.org/10.1016/j.yqres.2008.03.008>
- Spampinato, C.R., Costa, B., Di Stefano, A., Monaco, C., Scicchitano, G., 2011. The contribution of tectonics to relative sea-level change during the Holocene in coastal south-eastern Sicily: new data from boreholes. *Quaternary International*, 232, 214-227.  
<https://doi.org/10.1016/j.quaint.2010.06.025>
- Sulli, A., Gasparo Morticelli, M., Agate, M., Zizzo, E., 2021. Active north-vergent thrusting in the northern Sicily continental margin in the frame of the quaternary evolution of the Sicilian collisional system. *Tectonophysics*, 802, 1-18.  
<https://doi.org/10.1016/j.tecto.2021.228717>
- Temovski, M., Wieser, A., Marchhart, O., Braun, M., Madarász, B., Kiss, G. I., Palcsu, L., Ruzsicziczay-Rüdiger, Z., 2023. Pleistocene valley incision, landscape evolution and inferred tectonic uplift in the central parts of the Balkan Peninsula—Insights from the geochronology of cave deposits in the lower part of Crna Reka basin (N. Macedonia). *Geomorphology*, 445, 108994.  
<https://doi.org/10.1016/j.geomorph.2023.108994>
- Vattano, M., Audra, P., Bigot, J.-Y., De Waele, J., Madonia, G., Nobécourt, J.-C., 2012. Acqua fitusa cave: an example of inactive water-table sulphuric acid cave in central Sicily. *Rendiconti online della Società Geologica Italiana*, 21, 637-639.  
<https://www.researchgate.net/publication/235654140>
- Vattano, M., Audra, P., Benvenuto, F., Bigot, J.Y., De Waele, J., Galli, E., Madonia, G., Nobécourt J.C., 2013a. Hypogenic caves of Sicily (Southern Italy). In: Filippi, M., Bosak, P. (Eds.), *Proceedings of the 16th International Congress of Speleology*, Brno, 3, 144-149.  
<https://www.researchgate.net/publication/285808839>
- Vattano, M., Madonia, G., Audra, P., Bigot, J.-Y., De Waele, J., Nobécourt, J.-C., 2013b. Hypogenic caves in Sicily: a review. 21th International Karst School "Hypogene speleogenesis", Postojna. Karst Research Institute (IZRK), Poster.  
<http://dx.doi.org/10.13140/RG.2.2.19654.65604>
- Vattano, M., Scopelliti, G., Fulco, A., Presti, R., Sausa, L., Valenti, P., Di Maggio, C., Lo Valvo, M., Madonia, G., 2015. La Grotta dei Personaggi di Montevago (AG), una nuova segnalazione di cavità ipogenica in Sicilia. In: De Nitto, L., Maurano, M., Parise, M. (Eds.), *XXII Congresso Nazionale di Speleologia*, Memorie dell'Istituto Italiano di Speleologia, 2(29), 295-300.

- <https://www.researchgate.net/publication/277618027>  
Vattano, M., Madonia, G., Audra, P., D'Angeli, I.M., Galli, E., Bigot, J.-Y., Nobécourt, J.-C., De Waele, J., 2017. An overview of the hypogene caves of Sicily. In: Klimchouk, A.B., Palmer, A.N., Audra, P., De Waele, J., Auler, A. (Eds.), Hypogene karst regions and caves of the world. Springer, New York, p. 199-209.
- [http://dx.doi.org/10.1007/978-3-319-53348-3\\_1](http://dx.doi.org/10.1007/978-3-319-53348-3_1)  
Zupan-Hajna, N., 2003. Incomplete solution: Weathering of cave walls and the production, transport and deposition of carbonates fines. *Carsologica*. Založba ZRC, Ljubljana, 168 p. <https://doi.org/10.3986/9616358855>